BULLETIN OF CANADIAN PETROLEUM GEOLOGY
VOL. 55, NO. 1 (MARCH, 2007), P. 51–75

Shale gas potential of the Lower Jurassic Gordondale Member, northeastern British Columbia, Canada

DANIEL J.K. ROSS
Department of Geological Sciences
University of British Columbia
6339 Stores Road
Vancouver, BC V6T 1Z4
dross@eos.ubc.ca

R. MARC BUSTIN
Department of Geological Sciences
University of British Columbia
6339 Stores Road
Vancouver, BC V6T 1Z4

ABSTRACT

The Lower Jurassic Gordondale Member is an organic-rich mudrock and is widely considered to have potential as a shale gas reservoir. Influences of Gordondale mudrock composition on total gas capacities (sorbed and free gas) have been determined to assess the shale gas resource potential of strata in the Peace River district, northeastern British Columbia. Sorbed gas capacities of moisture-equilibrated samples increase over a range of 0.5 to 12 weight percent total organic carbon content (TOC). Methane adsorption capacities range from 0.05 cc/g to over 2 cc/g in organic-rich zones (at 6 MPa and 30ºC). Sorption capacities of mudrocks under dry conditions are greater than moisture equilibrated conditions due to water occupation of potential sorption sites. However, there is no consistent decrease of sorption capacity with increasing moisture as the relationship is masked by both the amount of organic matter and thermal maturation level. Clays also affect total gas capacities in as much as clay-rich mudrocks have high porosity which may be available for free gas. Gordondale samples enriched with carbonate (calcite and dolomite) typically have lower total porosities than carbonate-poor rocks and hence have lower potential free gas contents.

On a regional reservoir scale, a large proportion of the Gordondale total gas capacity is free gas storage (intergranular porosity), ranging from 0.1–22 Bcf/section (0.003–0.66 m^3/section). Total gas-in-place capacity ranges from 1–31.4 Bcf/section (0.03–0.94 m^3/section). The greatest potential for gas production is in the south of the study area (93-P) due to higher thermal maturity, TOC enrichment, higher reservoir pressure, greater unit thickness and improved fracture-potential.

RÉSUMÉ

Le Membre de Gordondale du Jurassique inférieur est un mudstone organique riche, et est généralement considéré comme présentant un potentiel de réservoir de gaz de schiste. Les influences de la composition du mudstone du Membre de Gordondale sur ses capacités en gaz total (gaz sorbé et gaz libre) ont été déterminées afin d'évaluer le potentiel de ressource en gaz de schiste des couches dans le district de Peace River, au nord-est de la Colombie Britannique. Les capacités en gaz sorbé d'échantillons, en teneur d'humidité équilibrée, augmentent sur une gamme allant de 0.5 à 12 pour cent du poids du contenu en carbone organique total (TCO). Les capacités d'adsorption du méthane vont de 0.05 cc/g à plus de 2 cc/g dans les zones organiques riches (à 6 MPa et 30ºC). Les capacités de sorption des mudstones, dans des conditions sèches, sont meilleures que dans des conditions d'humidité équilibrée, en raison de la présence d'eau dans les sites de sorption potentiels. Toutefois, il n'y a pas de diminution consistante de la capacité de sorption avec une augmentation de l'humidité, car cette relation se trouve masquée à la fois par la quantité de substance organique et le niveau de maturation thermale. La présence d'argiles affecte également les capacités de gaz total dans la mesure où les mudstones, riches en argile, présentent une haute teneur en porosité pouvant être disponible pour le gaz libre. Les échantillons de Gordondale, enrichis avec du carbonate (calcite et dolomie), présentent des porosités totales typiquement plus faibles que les roches pauvres en carbonate et, de ce fait, contiennent un potentiel plus faible en gaz libre.

A l'échelle du réservoir régional, une grande proportion de la capacité totale de gaz du Gordondale est l'accumulation de gaz libre (porosité intergranulaire), s'étalant sur 0.1–22 Bcf/section (0.003–0.66 m^3/section). La capacité de gaz total sur place s'étale sur 1–31.4 Bcf/section (0.03–0.94 m^3/section). Le plus important potentiel de production de gaz se trouve dans le sud de la zone étudiée (93-P) en raison de sa haute teneur en maturité thermale, de son enrichissement en TCO, des plus hautes pressions de réservoir, de sa plus grande épaisseur d'unité, et d'un meilleur potentiel de fracture.

Traduction de Gabrielle Drivet

Introduction

The success of unconventional gas production from gas shales[1] in the United States has sparked major interest in similar, organic-rich units in the Western Canadian Sedimentary Basin (WCSB). Gas shales are unique as the strata are both source and reservoir for the gas, and no apparent structural or stratigraphic traps are needed to retain the gas (USGS, 1995). Unlike conventional gas reservoirs, shale gas is stored in a number of ways including: 1) adsorbed to organic matter and clay particles; 2) as free gas in the rock pores and fractures; and 3) in solution within bitumen and water. However, due to the complex nature of gas storage, the detection, quantification and exploitation of unconventional reservoirs has proven difficult.

Studies undertaken in the United States identify total organic carbon content (TOC), maturity, mineral matter, porosity, permeability and thickness as the key parameters in assessment of gas shale resources (Harris et al., 1978; Cluff and Dickerson, 1982; Pollastro et al., 2003; Montgomery et al., 2005). However, due to the heterogeneity of shale gas reservoirs, relationships established for particular shales cannot be applied elsewhere. For example, from Appalachian Basin shales, Schettler and Parmoly (1990) argued gas adsorption was primarily associated with illite, and sorption onto kerogen was of secondary importance. Lu et al. (1995) also argued that despite low TOC values, significant adsorbed gas storage could be achieved due to methane adsorbing onto illite. Other shale gas research indicates a linear correlation between methane adsorption and TOC content (e.g. Lu et al., 1995; Ramos, 2004). Manger et al. (1991) suggested a positive relationship between TOC content and gas adsorption, but could only describe the association as qualitative.

The importance of natural fracture sets for gas production is also unclear. Natural fractures are essential for gas production in the Antrim Shale of the Michigan Basin (Manger et al., 1991), whereas permeable interbeds of siltstone are important in the Lewis Shale of the San Juan Basin (Bustin, 2005). In the absence of sufficient natural fracture sets and permeable horizons, induced fracturing can improve well performance (Montgomery et al., 2005). Hydraulically-induced fracturing has been most successful in the siliceous sections of the Barnett Shale, Fort Worth Basin, Texas (Pollastro et al., 2003), highlighting the need to consider the inorganic fraction for shale gas reservoir characterization and evaluation. Recent research from the Barnett Shale has also questioned the importance of pre-existing fractures due to the retardation of fracture stimulation by pre-existing natural fractures (Montgomery et al., 2005). Such findings emphasise the uniqueness and thus the importance of evaluating gas shale reservoirs on an individual basis.

The Lower Jurassic Gordondale Member is one of the most organic matter-rich units in the WCSB (Riediger et al., 1990; Riediger, 1991; Riediger and Bloch, 1995) and is considered a shale gas exploration target (Ross and Bustin, 2004). In this study, the relationship between mudrock composition and sorbed gas capacities from the Gordondale Member are reported. Shale samples from the overlying Poker Chip Shale are also included. The organic and inorganic fraction, moisture, thermal maturity and porosity are characterized to assess their effect on gas capacities. These results are combined with other Gordondale Member characteristics such as TOC, thickness and thermal maturity to evaluate the shale gas reservoir potential of the Gordondale Member in northeastern British Columbia (NE BC; Fig. 1).

Gordondale Member: Nomenclature, Stratigraphy and Composition

The Lower Jurassic Gordondale Member, the lowest unit of the Fernie Formation, forms the base of the Jurassic strata in the Peace River district, NE BC (Fig. 2). The Gordondale Member was deposited during transgression/regression cycles in a partially silled basin, created by terrane obduction onto the North American craton (Riediger et al., 1990; Riediger and Bloch, 1995). In NE BC and west-central Alberta, the Gordondale Member is the basinal equivalent of the lithologically and faunally different Nordegg Member in southwestern Alberta (see Frebold, 1957). The lithological and paleontological variability of the Gordondale/Nordegg members lead to a revision of the lower Fernie Formation nomenclature by Asgar-Deen et al. (2004) who proposed the Gordondale Member for the highly radioactive, Hettangian to upper Toarcian organic-rich strata in west-central Alberta and NE BC. In previous literature, Gordondale Member was referred to as the "Nordegg Member", differentiating Pliensbachian basinal deposits from the Nordegg in its type section (Alberta Foothills; e.g. Poulton et al., 1990; Riediger et al., 1990).

The Gordondale Member consists of mudstones, calcareous mudstones, phosphatic mudstones and phosphatic marlstones in NE BC, which are subdivided into four lithological units (Ross and Bustin, 2006). The only complete cored section of the Gordondale in NE BC is illustrated in Figure 3, highlighting the gamma-ray log response of the unit (75–250 API). More detailed organic petrology, inorganic geochemistry and sedimentological interpretation can be found in Ross and Bustin (2006), from which this data is summarized.

Unit A overlies Triassic strata of the Baldonnel, Pardonet and Charlie Lake. It consists of a conglomerate unit (up to 40 cm thick) but is not considered to have shale gas resource potential due to limited thickness (Ross, 2004). Unit B is a phosphatic, calcareous mudstone and marlstone unit, equivalent to Unit 1 of Asgar-Deen et al. (2003) and the Lower Radioactive Unit of Asgar-Deen et al. (2004). This interval has TOC contents ranging between 1 and 11 weight percent and gamma-ray responses up to 250 API. Quartz and calcite dominate the mineralogy with minor amounts of dolomite and clays. Unit C is a lower radioactive unit (gamma-ray approximately 75 API) composed of calcareous mudstones grading upwards to a siliceous mudstone (Unit 2 of Asgar-Deen et al., 2003 and Middle Silty Unit of

1 Gas shale is used in reference to fine-grained rocks in which a component of gas storage is by sorption. Gas shales are continuous-type natural gas reservoirs and are volumetrically important.

Asgar-Deen et al., 2004), with TOC between 6 and 21%. Calcite is dominant in the lower section and quartz in the upper section. Ross and Bustin (2006) show up to 94% of the silica is excess in unit C (silica which cannot be attributed to the detrital/clay fraction). The abundance of excess silica and the positive relationship between quartz and TOC suggest a biogenic source for the Si (Ross and Bustin, 2006). From their stratotype section in west-central Alberta, Asgar-Deen et al. (2004) described radiolarians within the Gordondale Member, attesting to the organic origin of at least a proportion of the silica. Unit D is a phosphatic marlstone to calcareous mudstone, with a slightly lower gamma-ray log response than unit B (maximum 225 API). Organic carbon contents range between 5 and 9%. The upper portion of unit D is clay-rich and silica is primarily associated with the clay component.

The contact between the Gordondale Member and the overlying Poker Chip Shale is marked by a thin conglomerate (Ross and Bustin, 2006). Riediger (2002) subdivided the Poker Chip Shale into units A and B (west-central Alberta). The organic-rich, oil-prone Poker Chip Shale A is equivalent to subunit 3A of Asgar-Deen et al. (2003) and unit D of the Gordondale in Ross and Bustin (2006). Poker Chip Shale B has little or no hydrocarbon generation potential and is equivalent to the grey-green fissile shale which overlies the Gordondale in NE BC (named Poker Chip Shale in this study).

In the 'typical' section of the Gordondale Member, NE BC, TOC enrichments are associated with lower gamma-ray log responses (Fig. 4). Uranium content, which is the primary control on Gordondale radioactivity (Ross and Bustin, 2006), is associated with P_2O_5 enrichments (Francolite, $Ca_{10}(PO_4)_6F_2$) and not TOC. The lack of U-TOC correlation is believed to represent partial dysoxic sedimentation of unit B and D where U is fixed by the phosphate ion (Ross and Bustin, 2006).

Natural fractures have been observed in conventional cores taken from the Gordondale Member (Ross, 2004). The majority of these fractures are calcite-filled, with some fractures showing an early calcite and later bitumen in-filling (Fig. 5).

Experimental

Samples

Thirty-eight samples (including four from the Poker Chip Shale) were taken from wells across the study area (Fig. 1) to assess the geologic controls on gas adsorption and total gas capacity. More detailed descriptions of all Gordondale cores in NE BC (see Fig. 1) are included in Ross (2004). Most cores only intersect the basal section of the Gordondale Member.

Methods

The concentrations of total carbon and sulphur content were determined by a Carlo Erba NA-1500 Analyzer for 38 mudrock, calcareous mudstone, marlstone and shale samples. Analytical precision was better than 2% for carbon and 5% for sulphur. Inorganic (carbonate) carbon concentration values

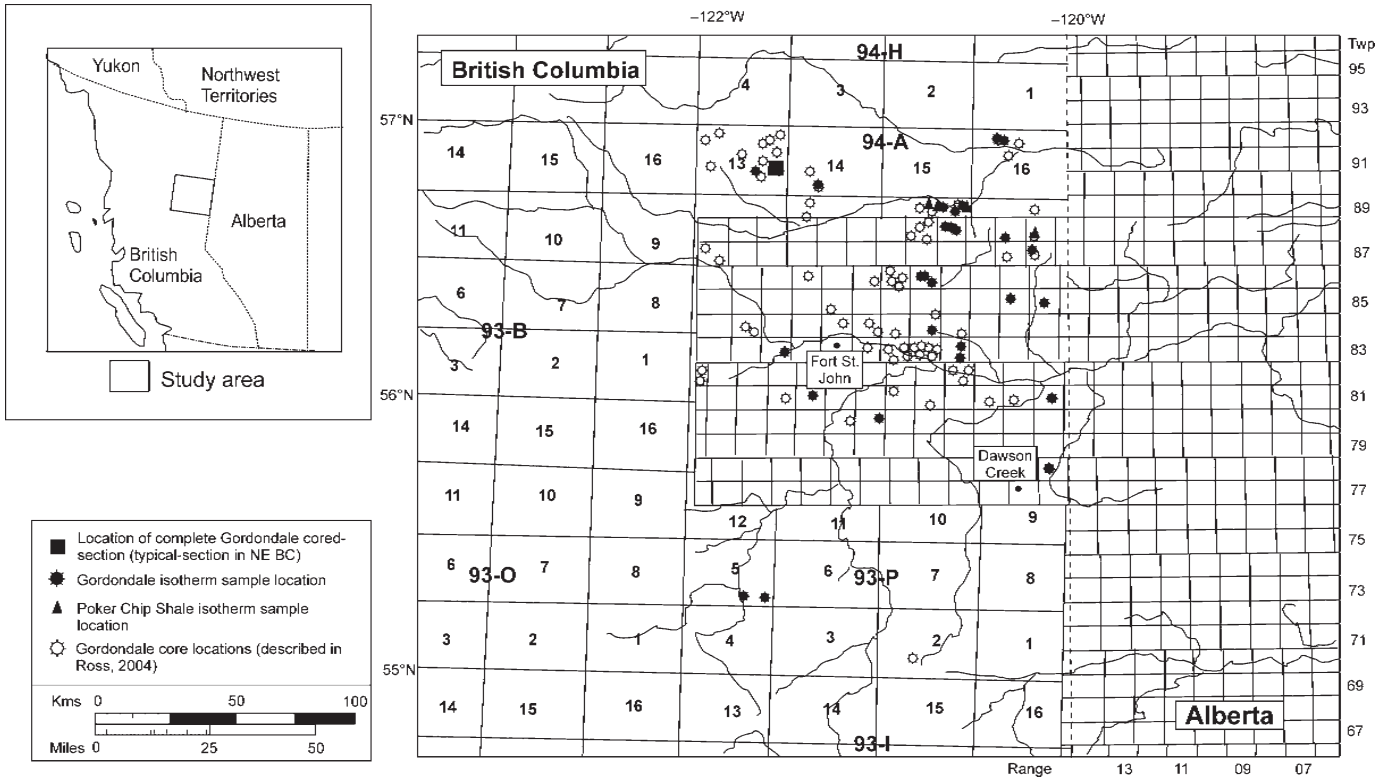

Fig.1. Map of northeastern British Columbia showing locations of Gordondale Member and Poker Chip Shale samples used in this study. Complete cored-section of the Gordondale Member (well: 200/d-088-H 094-A-13) and localities of Gordondale cores examined by Ross (2004) are also highlighted.

were determined using a CM5014 CO_2 coulometer by coulometric titration following release of CO_2 with 2 N $HClO_4$. Precision for total inorganic carbon is 2%. Total organic carbon was calculated as the difference between total and inorganic carbon values (i.e. TOC = TC–TIC). Elemental abundance of the samples was determined by X-ray fluorescence (XRF) for selected major elements (SiO_2, Al_2O_3, Fe_2O_3, K_2O, CaO, MgO, TiO_2, P_2O_5, Na_2O). Precision of results are ±3% for the major elements (except Na which is ±7%). Bulk mineralogy was determined by x-ray diffraction. Abundance of minerals were calculated semi-quantitatively using peak-area, corrected for Lorentz polarization (Pecharsky and Zavalij, 2003). Maturity data from Tmax by Rock Eval pyrolysis (Espitalié et al., 1977) was performed on pulverized samples using standard procedures on a Rock-Eval II/TOC apparatus. Hydrogen Indices (HI) are determined by the ratio of mg HC in S2/g TOC and Oxygen Indices (OI) are calculated from the ratio of mg CO_2 in S3/g TOC (Espitalié et al., 1977). Rock Eval Tmax values can be used to estimate the level of thermal maturity (Peters, 1986). However Rock Eval analyses only have significance for maturity and kerogen type above certain TOC and S2 values. If TOC contents are less than 0.3%, results are questionable, as are Tmax data when S2 values are less than 0.2 (Peters, 1986). Hence, all Rock Eval analyses have been examined and are deemed reliable if these guidelines are met, which also includes examination of the pyrograms to ensure Tmax values correspond to the kerogen peaks. Any questionable data is highlighted.

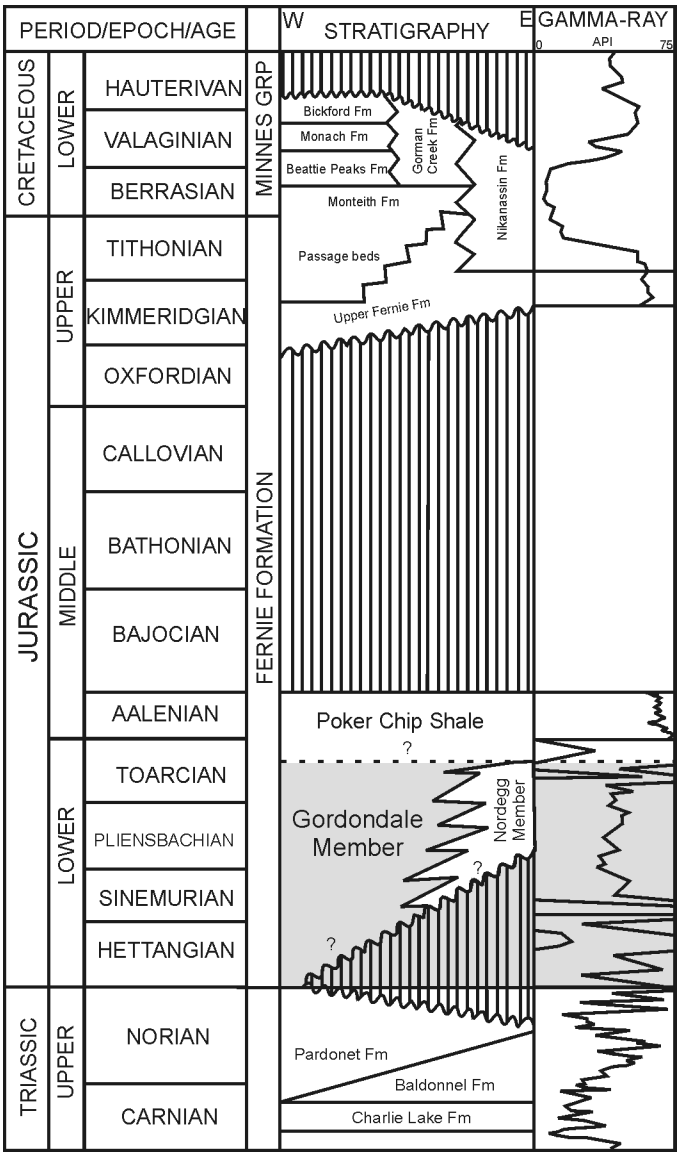

Fig. 2. Stratigraphic chart of Jurassic units in northeastern British Columbia (modified from Stott, 1967; Poulton et al., 1990; Riediger, 1990; Poulton et al., 1994; Asgar-Deen et al., 2004).

A volumetric, Boyles Law gas adsorption apparatus was used to measure high pressure methane isotherms at 30ºC. For each sample, pressure points were collected up to 9 MPa. Moisture equilibrated samples of 150 g were crushed to 250 μm in a ring-mill for adsorption analysis. Moisture capacities were determined by water saturation at 30ºC (ASTM, 2004) which is recommended for moisture content under reservoir conditions. The method consisted of equilibrating crushed shale samples over a saturated solution of potassium sulphate for more than 72 hours.

Total open pore volumes of mudrocks were determined using a Micromeritics Autopore IV 9500 Series®, calculated from the maximum volume of Hg penetrating at the highest pressure applied (206 MPa; Webb and Orr, 1997). Pore-size distributions (3–300 nm; Webb and Orr, 1997) were estimated by the intrusion of Hg at increasing pressures (0.004 MPa to 206 MPa in 45 pressure steps), utilizing the Washburn equation (Washburn, 1921). The samples were oven-dried at 110ºC for 1 hour prior to porosimetry analysis to remove all free and adsorbed moisture (Scromeda and Katsube, 1993).

Background: Adsorption Isotherms

In unconventional reservoirs, gas primarily exists in a condensed phase (liquid-density of the gas at boiling temperature at atmospheric pressure) due to physical adsorption. Physical adsorption is a weak, reversible attraction due to Van der Waals forces and is associated with a small heat of adsorption. When a gas adsorbs, it loses one of its three translational degrees of freedom. The kinetic energy lost by adsorption is converted to heat which is related to the heat of adsorption (see Gregg and Sing, 1982, for further discussion). Chemical absorption is far stronger, slower and irreversible (Yee et al., 1993) and the adsorbate is normally restricted to a monolayer. The volume of gas which can be stored in the sorbed state[2] is a function of pressure and temperature. A sorption isotherm gives a quantitative measure between the sorbate gas pressure and the amount of sorbate accommodated at a constant temperature. Five basic adsorption isotherms were described by Brunauer et al. (1940). Type I (Langmuir) is applied

2 Sorption is a general term which includes surface adsorption, absorption and capillary condensation (Greg and Sing, 1982).

to microporous materials which have a small external surface area such as organic matter in mudrocks. From the Type I isotherm, gas sorption increases rapidly at relatively low pressures whilst sorption sites are continuously filled. The steep initial slope of the isotherm is caused by the overlapping adsorption potential between the pore-walls, with the adsorbate gas molecule diameter only slightly smaller than the pores (Lowell and Shields, 1984). At higher pressures the system will reach saturation and no additional gas can be absorbed and a monolayer of adsorbate is produced and the isotherm flattens out.

The Langmuir Isotherm (Langmuir, 1918) can be written as:

$$V_E = \frac{V_L P}{P_L + P} \quad (1)$$

where V_E is the volume of absorbed gas per unit volume of the reservoir in equilibrium at pressure P_g, V_L is the Langmuir volume (based on monolayer adsorption), which is the maximum sorption capacity of the absorbent, P is the gas pressure and P_L is the Langmuir pressure which is the pressure at which total volume absorbed (V_E) is equal to one half of the Langmuir volume.

Sorption Isotherm Uses

Sorption analysis of gas shales is a critical element of reservoir analysis. There are three main uses:

1) To estimate the gas sorption capacity in situ.

2) To assess the source of the gas liberated (sorbed versus free gas) as reservoir pressure decreases through on-going production or pressure release/drawdown.

3) To determine the critical desorption pressure (CDP). The CDP is the pressure at which gas will begin to desorb. The difference between the CDP and the abandonment pressure is the total producible sorbed gas.

Results and Discussion

Organic and Inorganic Composition

Organic carbon contents range between 0.8–11.8% for the Gordondale Member and 0.8–2.2% for the Poker Chip Shale (Table 1). Sulphur contents vary between 1–4.8%. The Gordondale composition is dominated by variable amounts of

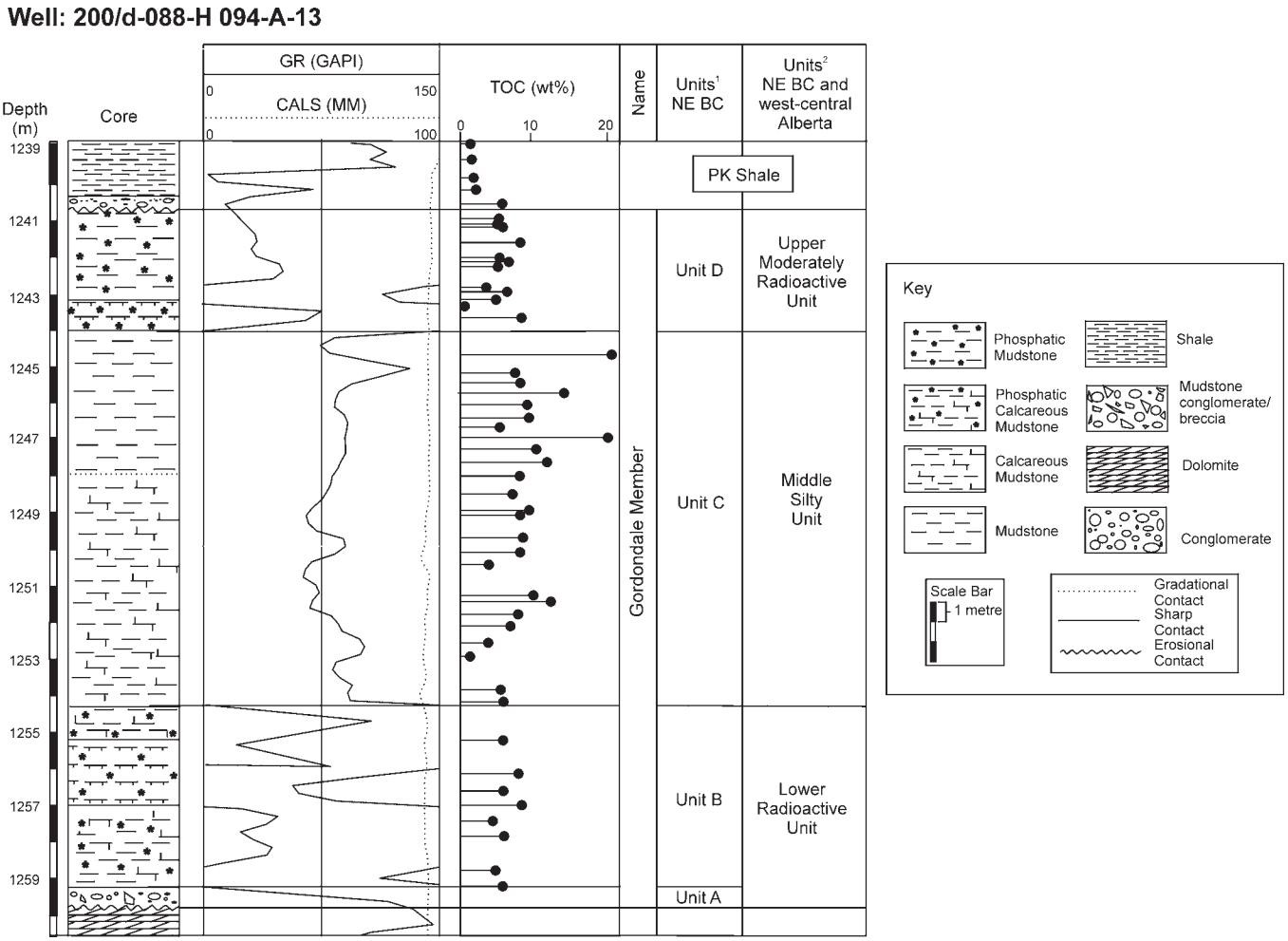

Fig. 3. Gamma-ray log, organic carbon contents and summarized core description for the Gordondale Member section in NE BC (200/d-088-H 094-A-13). Unit[1] classification from Ross and Bustin (2006) — see text for unit description summary. Unit[2] classification from Asgar-Deen et al. (2004) also shown. Detailed unit descriptions in Ross and Bustin (2006) and Asgar-Deen et al. (2003). GR=gamma ray in API units, CALS=calliper log in millimetres, PK=Poker Chip.

quartz, carbonate (primarily calcite with some dolomite) and clays (mainly illite), with lesser amounts of francolite, albite and pyrite (Tables 2 and 3). Poker Chip Shale samples are enriched in clays (inter-layers of illite-smectite) and quartz. Comparison of oxide and mineral data shows the difficulty of quantifying mineral phases based on XRD traces using peak areas. For example, from XRD[3] analysis, sample N2557-2 is composed of 91% quartz which is significantly higher than the SiO_2 content of 65% determined by XRF. Hence XRF data are used as proxies for mineral types (e.g. quartz, total clays, total carbonate; Figs. 6A–6D). The scatter of data points in the SiO_2 vs. quartz plot (Fig. 6A) highlights samples enriched in clay minerals.

Rock Eval Results

The organic fraction of the Gordondale in NE BC is dominated by Type I/II kerogen and smaller amounts of Type III kerogen (Table 4, Fig. 7). Despite the high TOC contents and predominance of hydrogen-rich liptinite macerals (alginite and matrix bituminite; Ross and Bustin, 2006), HI values are significantly lower than equivalent strata in west-central Alberta (up to 800 mg HC/g TOC; Riediger et al., 1990) most likely due to the greater level of thermal maturity of strata in NE BC (Table 4). As burial depth and maturation increases, HI values reduce as hydrocarbons are generated (maturation pathways shown as arrows on Fig. 7).

Rock Eval Tmax values of the Gordondale Member indicates excellent oil- to mixed oil-gas-prone source rock potential at moderate levels of thermal maturity. No immature Gordondale samples were encountered in this rock-suite with Tmax ranging from 441ºC to over 600ºC[4] (Table 4). Within the range of thermal maturities shown here, no relationship exists between maturity and TOC and variations in thermal maturity are not correlatable to mineralogy.

Methane Sorption and Organic Carbon

High pressure methane adsorption capacities for moisture-equilibrated Gordondale Member samples range from 0.05 cm^3/g in organic-poor samples to 2 cm^3/g for organic-rich samples (6 MPa and 30ºC at moisture equilibration; Table 1 and Fig. 8). Poker Chip Shale samples have lower sorbed gas capacities, with a maximum 0.21 cm^3/g (Table 1). The majority of methane isotherms for the Gordondale Member show a Langmuir-type isotherm up to 9 MPa. Occasionally, isotherms have a maximum adsorption capacity beyond these pressures, suggesting pores are only accessible at higher pressures causing

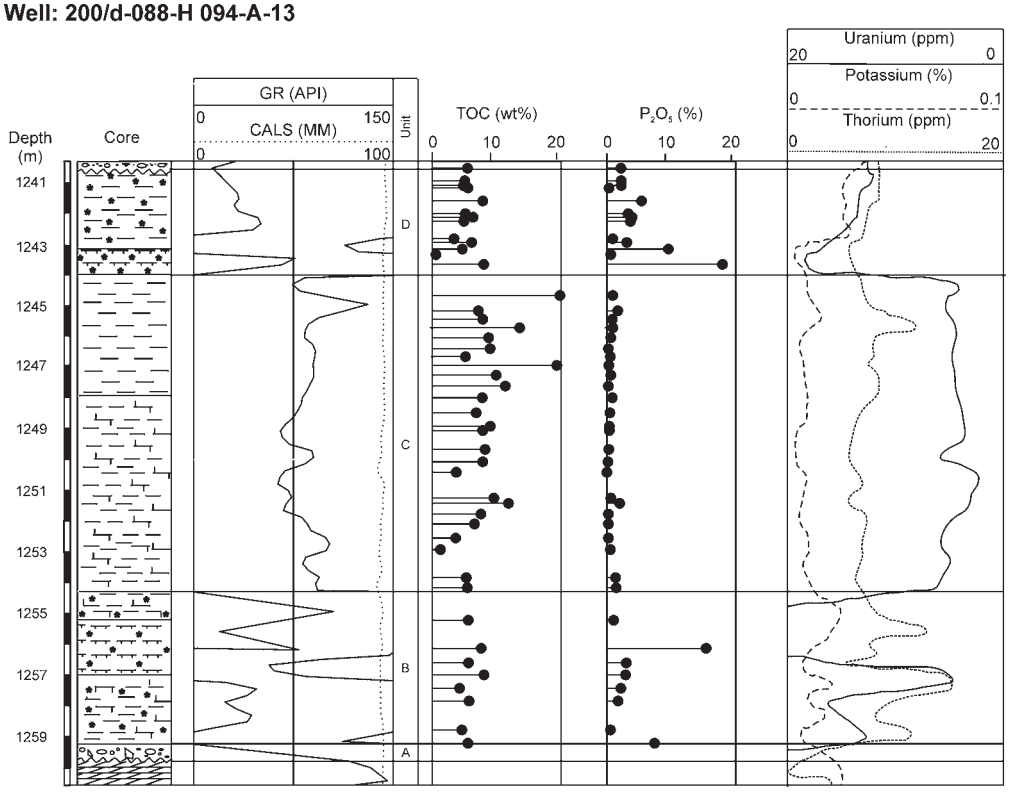

Fig. 4. Relationship between gamma-ray response, U and P_2O_5 concentrations in well 200/d-088-H 094-A-13. Note the gamma-ray log responds to U associated with the phosphatic mineral francolite and not to organic carbon contents.

3 Rietveld analysis for quantifying clays was not possible due to the presence of random interstratified clays in some samples.
4 Tmax values correspond to vitrinite reflectances (R_0) between 0.65% to over 3% (after Teichmüller and Durand, 1983).

deviation from the Langmuir equation (i.e. pores associated with restricted pore-throats). A weak, positive correlation between sorbed gas capacities and TOC concentrations ($r^2 = 0.39$; Fig. 9) indicates organic matter is in part responsible for adsorbing gas. Other possible factors that influence the relationship between TOC and gas sorption are discussed in later sections.

Larger sorbed gas capacities of moisture-equilibrated samples with increasing TOC are due to micropores[5] associated with the organic fraction, onto which gas can adsorb. Coals with greater micropore volumes have been shown to adsorb more gas compared to coals with more meso-macropores (e.g. Lamberson and Bustin, 1993). A solute gas component may also contribute to Gordondale sorbed gas capacities due to the potential solubilization of methane in amorphous/structureless matrix bituminite. Chalmers and Bustin (2007) show solubilization of methane is responsible for the large sorbed gas capacities of gilsonite and bituminite samples which have low surface area and micropore volumes compared to liptinite-poor coals. Using volumetric adsorption analysis, gas stored by adsorption cannot be differentiated from gas in solution.

Methane Sorption and Moisture Content

Gordondale Member equilibrium moisture contents range between 0.6 to 8.5%. Poker Chip Shale samples have moisture contents ranging between 5 and 11%. Although there is no apparent definitive relationship between sorbed gas capacity and moisture (Fig. 10A), samples with higher equilibrium moisture contents (>4%) tend to have a lower range of sorbed gas capacities (0.1–0.8 cm^3/g) than those with moisture contents less than 4% (0.1–2 cm^3/g sorbed methane). The variability of sorbed gas capacity of samples with less than 4% moisture is a result of different TOC contents (Fig. 10B). There are difficulties in assessing the relationship between organic matter (type and amount), moisture and sorption capacity as there are no organic-rich samples (e.g. >7% TOC) which have moisture contents greater than 4%.

Methane adsorption capacities of moisture-equilibrated samples in this study were up to 40% lower than those for dry samples (Fig. 11). By removing moisture, pore-throats are unblocked and additional adsorption sites are available to the methane molecule. The relationship of moisture content and methane capacity is quantified by comparing samples analyzed on a $EQ_{moisture}$ and dry basis, summarised as:

$$V_D = V_M (1+0.30m)$$

where V_D and V_M are the methane capacities for dry and $EQ_{moisture}$ shale samples and m is the moisture content. For comparison, Levy et al. (1997) suggested a multiplier of 0.39 for Bowen Basin coals from Australia whilst Ettinger et al. (1958) used 0.31. The larger multiplier for coals suggests a greater dependence of sorbed gas capacities to moisture in coal reservoirs compared to shale reservoirs — i.e. the percent

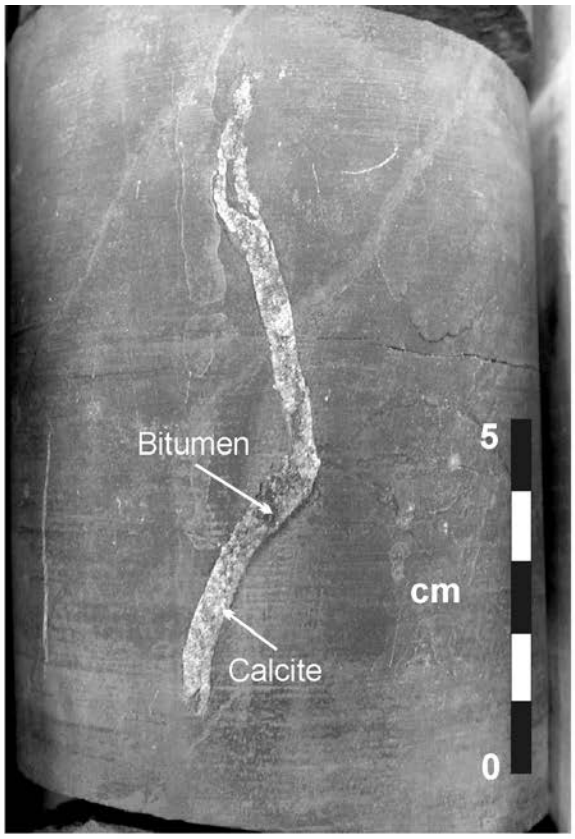

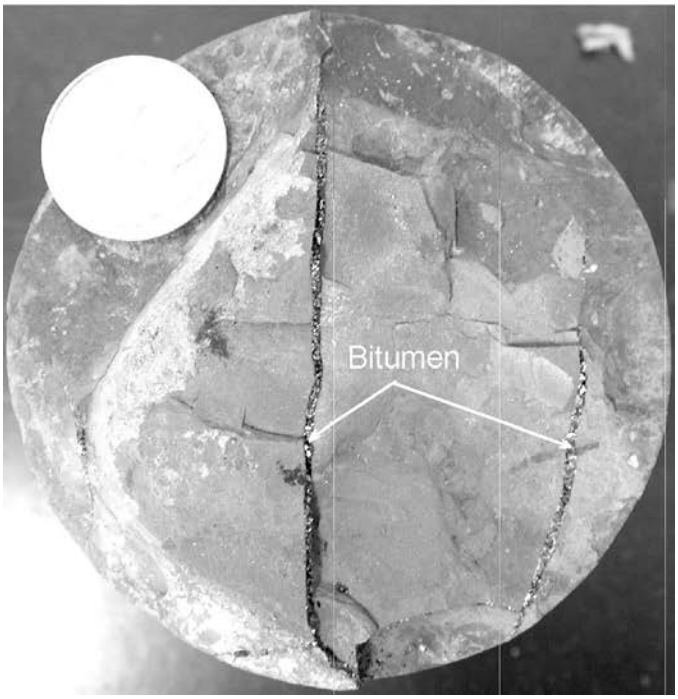

Fig. 5. Fractures of the Gordondale Member. A) Major vertical fracture with calcite and bitumen filling. B) Fractures with pure bitumen filling (viewed perpendicular to bedding; 25 cent coin for scale).

5 Porosity of microporous materials such as shales is classified according to size using the IUPAC classification: micropores (<2 nm), mesopores (2–50 nm) and macropores (>50 nm)

Table 1. Sorbed gas capacities, organic carbon contents (TOC), inorganic carbon contents (IC), sulphur contents (S) and equilibrium moisture contents of Gordondale (N) and Poker Chip Shale (PK) samples taken from NE BC. For comparison, Langmuir volumes determined at 6 MPa (SCF/ton = cc/g x 32.069).

Sample #	Well Location	Depth	TOC	IC	S	Moisture	Langmuir Volume @ 6MPa	
		(m)	(wt %)	(wt %)	(%)	(wt %)	(cc/g)	(scf/ton)
N154-1	00/12-31-078-14-W6/0	1713.9	9.2	3.9	-	1.4	1.36	43.6
N230-1	00/06-16-081-14-W6/0	1472.5	7.1	3.8	2.0	2.5	0.59	18.9
N230-2	00/06-16-081-14-W6/0	1484.9	10.7	3.7	-	1.8	1.40	44.9
N3098-3	00/11-30-087-14-W6/0	1179.8	9.6	2.7	3.2	1.8	0.76	24.4
N7912-1	00/13-28-085-15-W6/0	1253.3	6.6	5.4	-	1.2	0.70	22.4
N6738-2	00/06-05-088-15-W6/0	1083.2	7.4	0.2	-	2.7	0.79	25.3
N174-1	00/07-03-083-17-W6/00	1168.4	11.8	1.7	1.7	1.7	1.70	54.5
N49-2	00/10-25-083-17-W6/0	1268.6	10.0	2.6	-	2.3	1.52	48.7
N130-3	00/04-27-088-17-W6/0	1111.0	9.5	3.2	2.3	2.2	0.50	16.0
N1385-1	00/06-28-088-17-W6/0	1087.5	0.8	0.8	3.8	5.7	0.12	3.8
N2709-1	00/11-29-088-17-W6/0	1107.1	8.1	5.3	2.2	1.9	1.37	43.9
N72-1	00/04-03-084-18-W6/0	1248.0	6.9	3.6	2.6	3.2	0.69	22.0
N8153-1	00/02-02-086-18-W6/0	1129.0	10.5	4.8	2.3	1.7	0.59	18.9
N14270-2	100/10-30-086-18W6	1201.5	9.8	4.6	-	1.1	1.20	38.5
N8354-1	00/11-32-086-18-W6/0	1156.5	9.3	4.0	-	1.0	1.25	40.1
N91-1	00/16-36-080-20-W6/0	1630.2	10.2	1.8	1.0	0.6	0.96	30.8
N376-1	00/11-23-081-22-W6/0	1104.8	1.4	8.1	1.1	0.7	0.10	3.2
N108-1	00/01-12-084-23-W6/0	1134.7	3.6	2.6	1.4	1.6	0.76	24.4
N2557-2	00/c-074-J 094-A-10/0	1084.1	3.0	0.5	4.7	2.3	0.13	4.2
N5378-3	00/d-097-I 094-A-10/0	1112.0	9.4	0.6	-	2.0	1.10	35.3
N497-1	00/d-053-G 094-A-13/0	1284.0	6.7	3.4	-	5.9	0.50	16.0
N6080-1	00/d-088-H 094-A-13/0	1240.0	4.3	0.3	4.8	8.5	0.25	8.0
N6080-3	00/d-088-H 094-A-13/0	1250.1	7.5	4.3	1.6	1.8	0.53	17.0
N6080-5	00/d-088-H 094-A-13/0	1259.0	6.7	3.6	-	2.3	0.31	9.9
N6080-6	00/d-088-H 094-A-13/0	1244.9	5.6	0.3	-	1.8	0.44	14.1
N4941-1	00/d-075-I 094-A-13/0	1294.6	7.1	3.1	-	1.8	0.05	1.6
N89-1	00/b-078-C 094-A-14/0	1199.9	5.2	7.1	1.1	1.6	0.45	14.4
N9351-1	00/a-58-K 94-A-16/0	1013.1	3.1	0	2	3.7	0.82	26.3
N9682-1	00/a-73-K 94-A-16/0	1025.1	2.3	0.1	1.2	4.4	0.84	26.9
N3773-2	00/d-059-A 093-P-05/0	3425.9	5.0	1.2	1.7	1.7	1.16	37.2
N3793-1	00/a-065-B 093-P-05/0	2476.1	9.0	2.7	2.5	2.8	2.01	64.5
PK6738-1	00/06-05-088-15-W6/0	1081.0	1.0	0	3.6	4.8	0.18	5.8
PK5378-1	00/d-097-I 94-A-10/0	1102.5	0.8	0	4.4	10.9	0.15	4.8
PK2557-1	00/c-074-J 094-A-10/0	1082.0	1.0	0	4.7	6.7	0.21	6.7
PK2354-1	00/a-089-J 094-A-10/0	1059.0	2.2	0	4.7	5.0	0.15	4.8

Table 2. Major oxide data for Gordondale Member and Poker Chip Shale samples used in this study.

Sample #	Well Location	Depth	SiO_2	Al_2O_3	Fe_2O_3	CaO	K_2O	TiO_2	P_2O_5	MgO	Na_2O	LOI	Total
		m	%	%	%	%	%	%	%	%	%	%	%
N154-1	00/12-31-078-14-W6/0	1713.9	36.5	5.9	1.5	21.7	1.9	0.3	1.5	1.3	0.4	25.1	96.2
N230-1	00/06-16-081-14-W6/0	1472.5	42.7	11.3	4.5	14.3	1.5	0.4	0.4	1.0	1.7	21.8	100.0
N3098-3	00/11-30-087-14-W6/0	1179.8	28.1	6.9	3.1	22.4	2.4	0.4	0.7	3.6	0.3	26.7	94.8
N7912-1	00/13-28-085-15-W6/0	1253.3	24.4	7.1	2.1	27.1	2.3	0.3	2.1	2.0	0.3	26.0	93.8
N6738-2	00/06-05-088-15-W6/0	1083.2	65.1	8.4	4.0	1.6	1.5	0.5	0.6	1.2	0.4	15.9	99.0
N174-1	00/07-03-083-17-W6/00	1168.4	61.0	1.3	0.4	11.7	0.3	0.1	0.6	0.5	0.2	22.2	98.4
N49-2	00/10-25-083-17-W6/0	1268.6	38.0	7.6	2.3	18.2	2.8	0.4	0.6	2.1	0.4	25.6	98.1
N130-3	00/04-27-088-17-W6/0	1111.0	33.7	7.1	2.3	18.6	2.4	0.3	1.0	4.3	0.3	28.0	98.2
N1385-1	00/06-28-088-17-W6/0	1087.5	41.9	8.8	3.0	15.0	2.4	0.4	1.2	4.0	0.4	20.9	98.2
N2709-1	00/11-29-088-17-W6/0	1107.1	27.3	6.4	2.2	27.5	2.1	0.3	0.6	2.3	0.3	29.4	98.4
N72-1	00/04-03-084-18-W6/0	1248.0	38.7	6.9	2.4	19.7	2.4	0.3	1.1	1.7	0.4	22.7	96.3
N8153-1	00/02-02-086-18-W6/0	1129.0	27.5	6.7	2.0	24.8	2.0	0.3	0.6	1.3	0.3	28.5	94.3
N8354-1	00/11-32-086-18-W6/0	1156.5	44.0	5.0	2.1	17.9	0.7	0.2	1.0	1.1	0.5	26.1	98.8
N91-1	00/16-36-080-20-W6/0	1630.2	62.9	1.0	0.4	11.5	0.2	0.1	0.6	0.7	0.2	20.5	98.1
N376-1	00/11-23-081-22-W6/0	1104.8	18.8	3.2	1.5	24.5	1.2	0.2	1.5	15.9	0.2	31.6	98.6
N108-1	00/01-12-084-23-W6/0	1134.7	46.1	9.6	2.1	13.2	3.0	0.6	1.7	4.1	0.8	17.2	98.4
N2557-2	00/c-074-J 094-A-10/0	1084.1	65.0	4.0	5.9	6.7	0.6	0.2	3.4	1.3	0.3	10.7	98.3
N5378-3	00/d-097-I 094-A-10/0	1112.0	66.1	5.9	2.1	4.9	1.0	0.3	0.9	1.1	0.5	16.8	99.5
N497-1	00/d-053-G 094-A-13/0	1284.0	37.1	7.8	2.5	17.1	2.7	0.4	0.6	4.8	0.4	24.8	98.1
N6080-1	00/d-088-H 094-A-13/0	1240.0	54.9	15.2	6.4	1.2	3.3	0.7	0.2	1.8	0.6	15.3	99.7
N6080-3	00/d-088-H 094-A-13/0	1250.1	46.4	4.4	1.1	19.2	0.7	0.2	0.7	1.2	0.5	23.6	98.2
N89-1	00/b-078-C 094-A-14/0	1199.9	16.8	5.5	1.4	35.0	1.4	0.2	2.6	1.2	0.2	29.3	93.9
N9351-1	00/a-58-K 94-A-16/0	1013.1	62.4	16.5	3.1	0.8	4.4	0.9	0.3	1.2	0.5	9.5	99.7
N9682-1	00/a-73-K 94-A-16/0	1025.1	65.4	16.1	2.4	0.5	3.6	0.9	0.3	1.1	0.4	8.3	99.4
N3773-2	00/d-059-A 093-P-05/0	3425.9	63.9	5.8	1.6	8.6	1.2	0.1	2.0	1.5	0.5	13.0	98.2
N3793-1	00/a-65-B 93-P-05/0	2476.1	47.3	8.5	2.5	13.8	1.3	0.2	0.4	0.9	1.0	22.9	99.0
PK6738-1	00/06-05-088-15-W6/0	1081.0	60.0	17.8	5.8	0.1	2.2	0.9	0.0	0.9	0.4	11.8	100.1
PK5378-1	00/d-097-I 94-A-10/0	1102.5	53.5	18.4	6.4	0.1	3.5	0.9	0.1	1.7	0.6	14.6	99.9
PK2557-1	00/c-074-J 094-A-10/0	1082.0	53.4	18.2	6.9	0.3	3.3	0.8	0.1	1.8	0.7	13.7	99.4
PK2354-1	00/a-089-J 094-A-10/0	1059.0	56.3	19.8	5.5	0.3	2.6	1.0	0.2	1.2	0.6	12.2	99.8

Table 3. Relative mineral abundances of Gordondale samples examined for sorbed gas capacity. *Poker Chip Shale samples dominated by interstratified illite-smectite (reported as illite concentration).

Sample #	Well Location	Depth	Francolite	Illite	Kaolinite	Quartz	Pyrite	Calcite	Dolomite	Albite	Total Carbonate	Total Clays
		m	%	%	%	%	%	%	%	%	%	%
N154-1	00/12-31-078-14-W6/0	1713.9	0.6	17.9	0.0	39.5	0.8	37.7	2.2	0.0	39.9	17.9
N230-1	00/06-16-081-14-W6/0	1472.5	0.6	28.1	0.0	31.3	0.0	37.2	1.3	2.2	38.4	28.1
N3098-3	00/11-30-087-14-W6/0	1179.8	0.6	42.4	0.0	21.1	0.0	26.5	7.8	0.4	34.3	42.4
N7912-1	00/13-28-085-15-W6/0	1253.3	0.6	34.7	0.0	19.0	1.3	40.9	2.7	0.0	43.6	34.7
N6738-2	00/06-05-088-15-W6/0	1083.2	0.6	17.5	0.0	80.0	1.5	0.0	1.0	0.0	1.0	17.5
N174-1	00/07-03-083-17-W6/00	1168.4	0.6	0.0	0.0	83.3	0.0	16.0	0.7	0.0	16.7	0.0
N49-2	00/10-25-083-17-W6/0	1268.6	0.6	40.0	0.0	32.6	1.0	22.0	3.9	0.5	25.9	40.0
N130-3	00/04-27-088-17-W6/0	1111.0	0.6	31.4	0.0	31.4	1.0	22.0	10.0	3.0	32.0	31.4
N1385-1	00/06-28-088-17-W6/0	1087.5	0.6	48.0	0.0	27.0	1.1	20.0	2.9	0.0	22.9	48.0
N72-1	00/04-03-084-18-W6/0	1248.0	0.6	49.4	0.0	27.3	0.8	19.3	1.7	0.4	21.0	49.4
N8153-1	00/02-02-086-18-W6/0	1129.0	0.6	37.8	0.0	20.8	0.7	38.5	1.5	0.8	39.9	37.8
N8354-1	00/11-32-086-18-W6/0	1156.5	0.6	13.4	0.0	52.2	1.3	31.7	1.4	0.0	33.1	13.4
N91-1	00/16-36-080-20-W6/0	1630.2	0.6	0.0	0.0	83.0	0.0	15.5	1.5	0.0	17.0	0.0
N376-1	00/11-23-081-22-W6/0	1104.8	0.6	13.2	0.0	22.1	0.0	0.0	64.8	0.0	64.8	13.2
N108-1	00/01-12-084-23-W6/0	1134.7	0.6	48.0	0.0	30.0	1.4	8.3	8.1	2.0	16.3	48.0
N2557-2	00/c-074-J 094-A-10/0	1084.1	0.6	0.0	0.0	91.8	3.8	0.0	2.4	0.0	2.4	0.0
N5378-3	00/d-097-I 094-A-10/0	1112.0	0.6	21.7	0.0	73.1	1.0	3.0	0.0	0.0	3.0	21.7
N497-1	00/d-053-G 094-A-13/0	1284.0	0.6	33.4	0.0	36.8	1.1	17.1	11.6	0.0	28.7	33.4
N6080-1	00/d-088-H 094-A-13/0	1240.0	0.6	62.9	0.9	30.8	1.1	0.0	1.0	0.0	1.0	63.8
N89-1	00/b-078-C 094-A-14/0	1199.9	0.6	28.7	0.0	10.4	0.0	54.9	2.9	0.0	57.9	28.7
N9351-1	00/a-58-K 94-A-16/0	1013.1	0.6	72.7	0.0	27.3	0.0	0.0	0.0	0.0	0.0	72.7
N3773-2	00/d-059-A 093-P-05/0	3425.9	0.6	26.2	0.0	67.2	0.0	4.6	2.0	0.0	6.6	26.2
N3793-1	00/a-65-B 93-P-05/0	2476.1	0.6	42.1	0.0	36.3	1.2	17.7	0.1	2.6	17.9	42.1
PK6738-1	00/06-05-088-15-W6/0	1081.0	0.6	50.7*	32.5	16.2	0.7	0.0	0.0	0.0	0.0	83.2
N5378-1	00/d-097-I 94-A-10/0	1102.5	0.6	78.2*	4.5	16.3	1.0	0.0	0.0	0.0	0.0	82.7
PK2354-1	00/a-089-J 094-A-10/0	1059.0	0.6	60.3*	15.4	21.8	0.7	1.8	0.0	0.0	1.8	75.7

reduction of sorbed gas capacity on dry to moisture equilibrated samples is larger for coals.

Methane Sorption and the Influence of Mineral Matter

Quartz and calcite, which accounts for 60–90% of mineral phases of the Gordondale sample set, have low internal surface areas and hence have low sorption capacity. Clays have significant surface areas and may adsorb methane to their internal structure (Valzone et al., 2002; Venaruzzo et al., 2002), as has been argued for Devonian shale gas reservoirs in the US (Lu et al., 1995). In this study however, there is no correlation between Al_2O_3 (proxy for clay content) and sorbed gas capacity (r^2 = 0.01) under moisture equilibrated conditions, thus methane sorption to clays is of minimal importance when saturated with water. The low sorption capacities of clays relate to the affinity of water to their negatively charged surfaces (Figure 12; Chiou and Rutherford, 1997), removing a large proportion of potential surficial sorption sites.

The greater equilibrium moisture contents of the Poker Chip Shale samples (5–11% moisture compared to 2.6% average for Gordondale samples) can be attributed to the larger aluminosilicate fraction (17–20% compared to 7.4% average for Gordondale). The presence of interstratified smectite-illite in the Poker Chip Shales can cause a marked increase in moisture contents (PK5378-1) relative to comparable Al_2O_3 concentrations of Gordondale samples which contain no smectite (only illite and kaolinite). Smectite equilibrium moisture content is 18% as compared to illite (3%) and kaolinite (7%; Ross, 2004) due to the increase of water adsorption on high charged smectites (Chiou and Rutherford, 1997; Laird, 1999). Coeval enrichment of clays and moisture has also been reported for coals. McCutcheon and Barton (1999) investigated the relationship between clay content and moisture capacities in a suite of bituminous coals reporting moisture contents 2.3–2.8 times greater for mineral matter than that of the organic matter. Coal mineral matter enriched in montmorillonite had double the moisture capacity of coals in which the only clay present was kaolinite.

Methane Sorption and Thermal Maturity

In Figure 13, the relationship between TOC and methane adsorption is plotted for a range of thermal maturities as represented by Tmax. Although there is an increase in sorbed gas capacities with greater thermal maturity (e.g. samples N3773-2 and N3793-1), there is no significant linear correlation between Tmax and sorption. The higher sorbed gas capacities of high

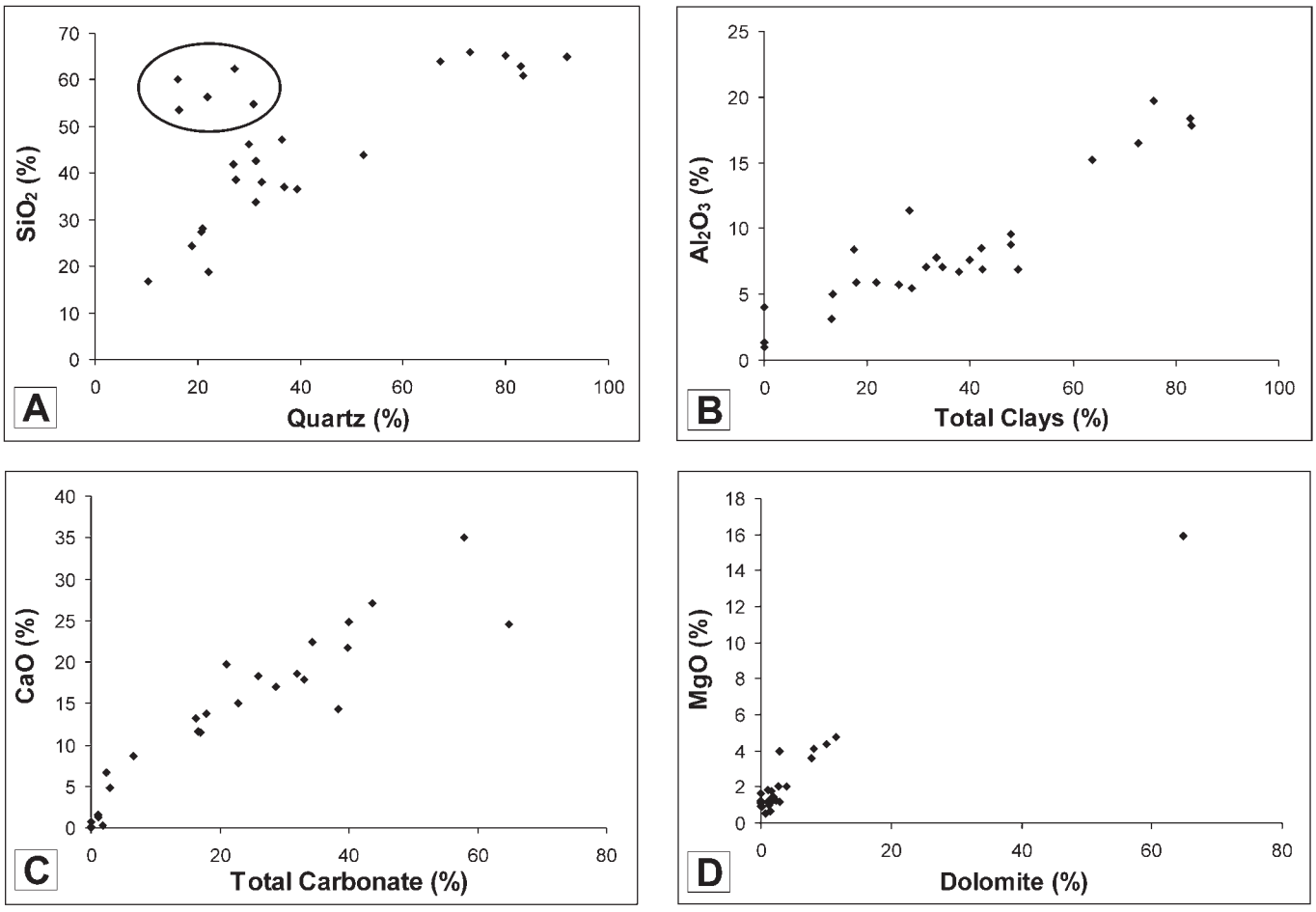

Fig. 6 A–D. Correlations of major oxide data (determined by XRF) and mineralogy (determined by XRD) for Gordondale isotherm samples used in this study. Note abundant SiO_2 relative to quartz in some samples due to larger clay mineral fraction.

Table 4. Rock Eval pyrolysis data for selected Gordondale and Poker Chip samples. S1 and S2 (mg hydrocarbons/gram Rock); Hydrogen Index (HI = S2/TOCx100) and Oxygen Index (OI = [mg CO_2/gm sample/TOC); PI = S1/ (S1+S2).
Note: samples asterisked are considered questionable following recommendations by Peters (1986).

Sample #	Well Location	Depth (m)	Tmax (°C)	S1	S2	S3	PI	S2/S3	HI	OI
N154-1	00/12-31-078-14-W6/0	1713.9	479	0.91	5.23	0.33	0.15	15.85	56	4
N230-1	00/06-16-081-14-W6/0	1472.5	447	2.37	14.43	0.30	0.14	48.10	225	5
N3098-3	00/11-30-087-14-W6/0	1179.8	441	1.89	12.95	0.34	0.13	38.09	192	5
N7912-1	00/13-28-085-15-W6/0	1253.3	450	1.75	10.01	0.32	0.15	31.28	171	5
N6738-2	00/06-05-088-15-W6/0	1083.2	441	2.65	17.12	0.29	0.13	59.03	231	4
N174-1	00/07-03-083-17-W6/00	1168.4	459	5.66	19.00	0.23	0.23	82.61	169	2
N49-2	00/10-25-083-17-W6/0	1268.6	461	1.38	9.72	0.33	0.12	29.45	99	3
N130-3	00/04-27-088-17-W6/0	1111.0	448	1.77	19.01	0.35	0.09	54.31	219	4
N1385-1	00/06-28-088-17-W6/0	1087.5	463	0.76	2.14	0.21	0.26	10.19	55	5
N2709-1	00/11-29-088-17-W6/0	1107.1	445	1.34	18.69	0.30	0.07	62.30	230	4
N72-1	00/04-03-084-18-W6/0	1248.0	458	1.09	5.51	0.36	0.17	15.31	76	5
N8153-1	00/02-02-086-18-W6/0	1129.0	453	2.34	13.14	0.37	0.15	35.51	131	4
N8354-1	00/11-32-086-18-W6/0	1156.5	454	3.00	15.26	0.30	0.16	50.87	164	3
N91-1	00/16-36-080-20-W6/0	1630.2	467	5.05	11.95	0.44	0.30	27.16	122	5
N376-1*	00/11-23-081-22-W6/0	1104.8	494	0.05	0.24	0.19	0.18	1.26	40	32
N108-1	00/01-12-084-23-W6/0	1134.7	473	0.67	1.85	0.25	0.27	7.40	62	8
N2557-2	00/c-074-J 094-A-10/0	1084.1	442	0.94	4.67	0.20	0.17	23.35	170	7
N5378-3	00/d-097-I 094-A-10/0	1112.0	446	3.05	29.10	0.20	0.09	145.50	320	2
N497-1	00/d-053-G 094-A-13/0	1284.0	472	0.40	2.57	0.25	0.14	10.28	52	5
N6080-1	00/d-088-H 094-A-13/0	1240.0	462	0.41	1.63	0.37	0.20	4.41	37	8
N6080-3	00/d-088-H 094-A-13/0	1250.1	464	4.36	8.11	0.23	0.35	35.26	113	3
N89-1	00/b-078-C 094-A-14/0	1199.9	457	1.47	6.10	0.47	0.19	12.98	138	11
N9351-1	00/a-58-K 94-A-16/0	1013.1	451	0.93	9.01	0.13	0.09	69.31	291	4
N9682-1	00/a-73-K 94-A-16/0	1025.1	447	0.54	6.64	0.10	0.08	66.40	293	4
N3773-2	00/d-059-A 093-P-05/0	3425.9	608	0.25	0.25	0.26	0.50	0.96	5	5
N3793-1	00/a-065-B 093-P-05/0	2476.1	607	0.04	0.31	0.41	0.12	0.76	4	5
N6738-1	00/06-05-088-15-W6/0	1081.0	429	0.27	0.24	0.14	0.53	1.71	32	18
PK5378-1*	00/d-097-I 94-A-10/0	1102.5	425	0.27	0.15	0.21	0.64	0.71	25	36
PK2557-1	00/c-074-J 094-A-10/0	1082.0	428	0.47	0.30	0.12	0.61	2.50	41	16
PK2354-1	00/a-089-J 094-A-10/0	1059.0	454	0.52	2.50	0.12	0.17	20.83	110	5

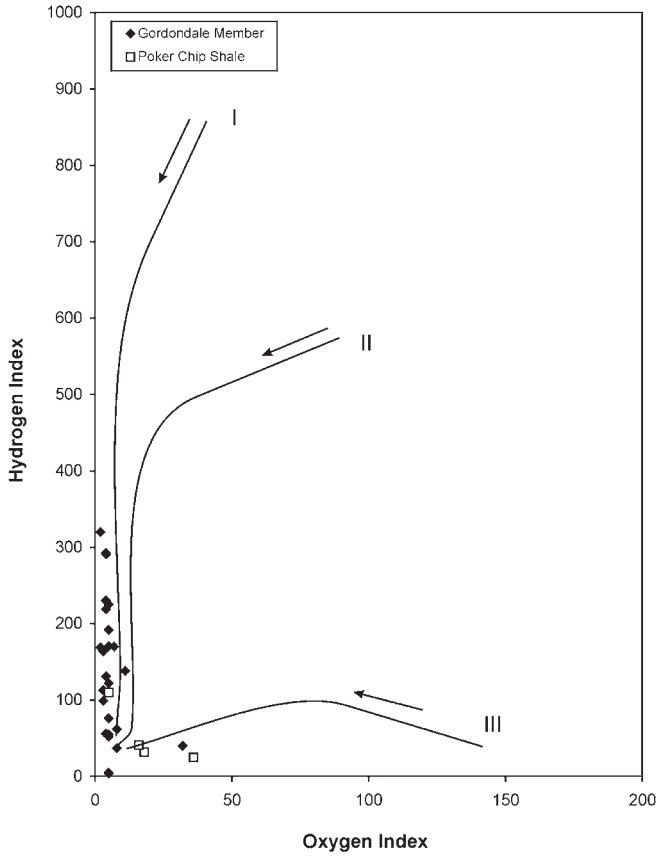

Fig. 7. Hydrogen Index vs. Oxygen Index for isotherm samples of the Gordondale Member. Classification of kerogen types I–III are shown. Arrows indicate maturation pathways where more mature samples plot closer to the origin.

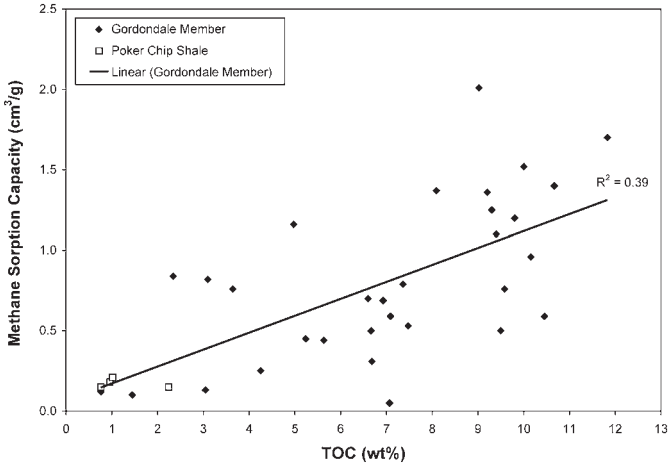

Fig. 9. Plot of methane capacity at 6 MPa with varying TOC contents. Poor–moderate correlation between methane sorption and TOC suggests other factors influence the organic-gas sorption relationship.

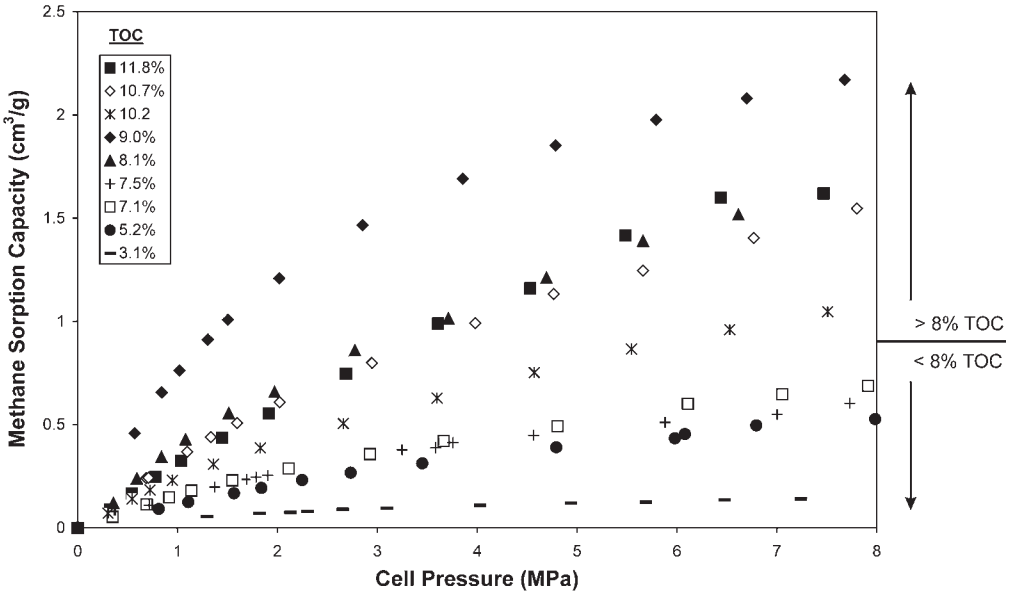

Fig. 8. Variation in high pressure methane sorption isotherms with organic carbon contents from the Gordondale Member. Samples show a general increase in sorption capacity with TOC but some isotherms do not show a typical Type I isotherm.

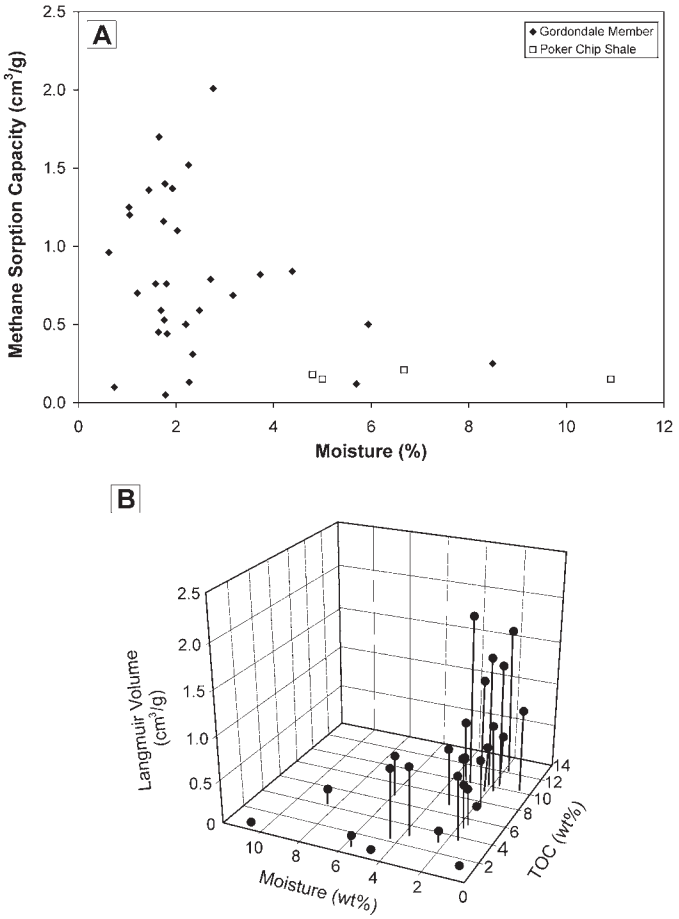

Fig. 10. Moisture and sorption capacity. A) Correlation between sorption capacity and moisture. Note lack of high sorption capacities in moisture-rich samples. B) Three-dimensional plot of TOC, moisture and sorbed gas capacity. Larger sorbed gas capacities are associated with organic-rich samples and moisture contents less than 4%. The data become scattered when TOC contents are low and moisture contents are more variable.

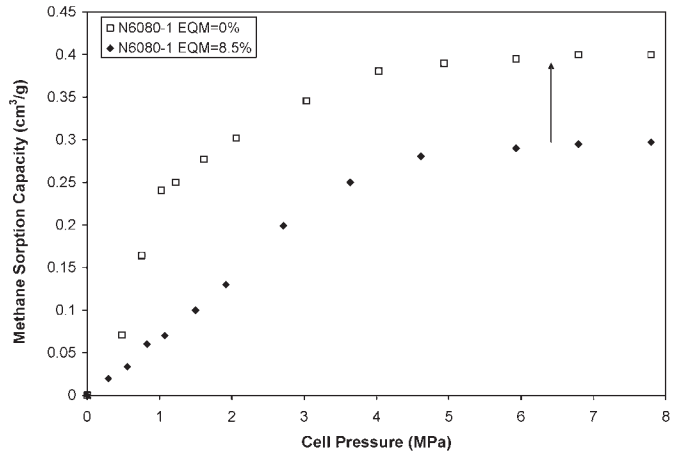

Fig. 11. Change of methane sorption capacity of sample N6080-1 under dry- and moisture-equilibrated conditions (EQM=equilibrated moisture contents).

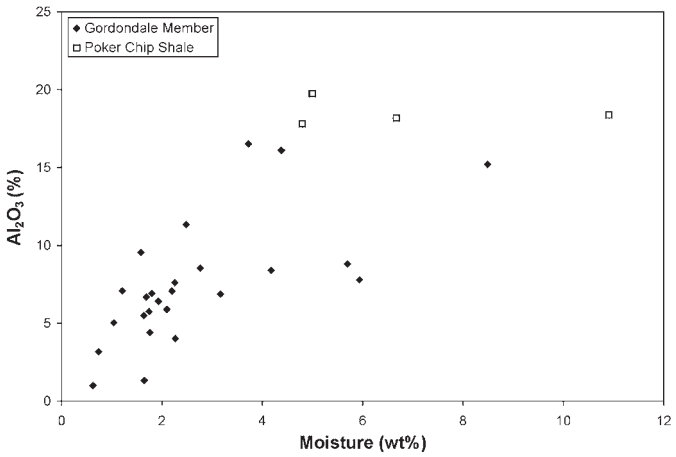

Fig. 12. Correlation of equilibrium moisture content with aluminosilicates (r^2=0.6 for Gordondale Member samples), underlining the importance of the clay fraction in mudrocks and shales to moisture capacities.

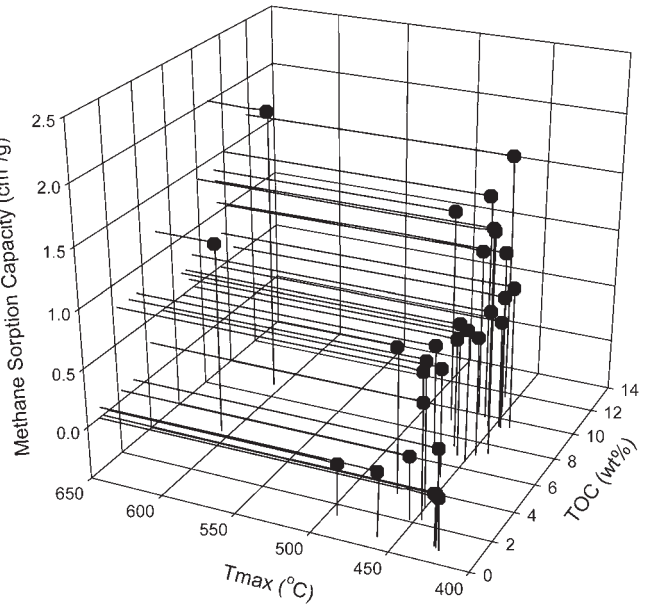

Fig. 13. 3-D plot of TOC, maturity and sorption capacity. Note larger sorbed gas capacities of samples >600°C Tmax compared to samples with comparable TOC but lower thermal maturities (<500°C Tmax).

Tmax samples N3773-2 and N3793-1, compared to samples with lower Tmax values but similar TOC and moisture contents, may be related to structural transformation of the organic fraction. Laxminarayana and Crosdale (1999) argue pore surface heterogeneities of the organic matter decreases in coals (due to increased aromaticity) with increasing rank, which allow more complete coverage of the internal surfaces by gas molecules. The lack of Tmax data between 500 and 600ºC for the Gordondale samples restricts assessing the influence of maturity on gas sorption in this study.

Porosity and Free Gas

The integration of total porosity data (free gas potential) with sorbed gas capacities provides a measure of the maximum potential maximum gas capacity for determining the economic feasibility of the shale gas reservoir. Total porosities range between 0.5 and 4.2% for the Gordondale Member (Table 5) and 5.4 and 6.1% for two Poker Chip Shale samples. A porosity of 0.5% saturated with gas (S_w=0) only accounts for approximately 5% of the total gas capacity (Fig. 14A), whereas a sample with 4.2% porosity (Fig. 14B) has an estimated free-gas capacity which constitutes up to 50% of the total gas content.

Porosity increase with increasing aluminosilicate abundance underscores the influence of lithology on total porosity and pore-size distribution in mudrocks and shales. For example, Poker Chip Shale samples have high porosity and highest clay content (Fig. 15A). Rieke and Chilingarian (1974) found clay minerals may still have porosity values of 25% at a stress equivalent to 5 km overburden, despite their compressible nature. Bjørlykke (1999) suggested the lack of pore-reduction of clays is due to the large surface area of fine clay particles and associated bound water. As such, clays may be the most significant contributor to total porosity in fine-grained sediments.

Conversely, abundance of carbonate is negatively correlated with total porosity of the Gordondale Member (Fig. 15B). Mercury porosimetry analysis also reveals the inability of Hg to penetrate the micropores of carbonate-rich samples, with average pore-size of about 90, 000 nm (sample N89-1, Fig. 16). Calcite within the Gordondale Member, consisting of planar or continuous fibrous calcite, precipitated during early-stage diagenesis (Riediger and Coniglio, 1992) and may have reduced porosity through pore-cementation. Clay-rich samples tend to have unimodal pore-size distributions in the 10 nm range (e.g. N9351-1; Fig. 16) with occasional secondary modes within a larger pore-throat size. These results are similar to previous pore-size distribution data on mudrock and shale sequences (Katsube and Williamson, 1994; Dorsch and Katsube, 1999). Microporosity associated with the organic fraction is not shown (<2 nm diameter) since the smallest pore diameter measurable using Hg porosimetry is 3 nm.

With greater burial depth (and associated higher temperature and subsequent diagenesis), compaction reduces mudrock porosity (e.g. Issler, 1992; Aplin et al., 1995) and may account for the lower porosity of N3773-2 (Tmax 608ºC and depth of 3425.9 m – highlighted in Figs. 15A, 15B and 16). Porosity as a function of thermal maturity is shown in Figure 17, demonstrating that pore-reduction through compaction (proxied by Tmax values aside of heat flow variability) only partly explains the porosity variability.

Shale Gas Reservoir Evaluation

The amount, type and thermal maturity of organic carbon, thickness, producibility and total gas capacities are examined

Table 5. Skeletal density, bulk density and total porosity of Gordondale and Poker Chip Shale samples (measured by Hg porosimetry). Samples selected on the basis of inorganic geochemistry and thermal maturity variability.

Sample #	Well Location	Depth (m)	TOC (%)	Skeletal Density (g/cm^3)	Bulk Density (g/cm^3)	Porosity (%)
N230-1	00/06-16-081-14-W6/0	1472.5	7.1	2.47	2.42	2.20
N49-2	00/10-25-083-17-W6/0	1268.6	10	2.48	2.44	1.52
N2709-1	00/11-29-088-17-W6/0	1107.1	8.1	2.47	2.41	2.11
N91-1	00/16-36-080-20-W6/0	1630.2	10.2	2.34	2.25	4.17
N376-1	00/11-23-081-22-W6/0	1104.8	1.4	2.80	2.78	0.50
N2557-2	00/c-074-J 094-A-10/0	1084.1	3.1	2.57	2.50	2.62
N6080-1	00/d-088-H 094-A-13/0	1240.0	4.3	2.61	2.54	2.77
N6080-3	00/d-088-H 094-A-13/0	1250.1	7.5	2.41	2.30	3.90
N89-1	00/b-078-C 094-A-14/0	1199.9	5.2	2.57	2.55	0.82
N9351-1	00/a-058-K 94-A-16/0	1013.1	3.1	2.58	2.49	3.41
N3773-2	00/d-059-A 093-P-05/0	3425.9	5.0	2.55	2.54	0.50
PK5378-1	00/d-097-I 94-A-10/0	1102.5	0.8	2.43	2.30	6.10
PK2354-1	00/a-089-J 094-A-10/0	1059.0	2.2	2.67	2.53	5.40

to assess regional reservoir trends of the Gordondale Member in NE BC and identify areas with exploration potential.

Gordondale Organic Matter

Total organic carbon values for samples collected from the Gordondale range between 0.8 and 22% (this study and Ross and Bustin, 2006) but TOC contents of up to 40% occur locally (Ross, 2004). Organic-rich regions are, in part, associated with thicker sections of the Gordondale along the NW–SE section of the study area (Fig. 18; Ross, 2004) with maximum TOC values in the SW part of the study area (93-P-03).

Thermal Maturity

On a regional scale, Tmax ranges between 435ºC in the northeast to greater than 600ºC in the south (Bustin, 1990) where the Gordondale is in the dry gas window (Fig. 19). In the thermally over-mature areas, large quantities of gas may still have potential to occur/exist, primarily from secondary cracking of in-situ oils (Hunt, 1996). Similarly in the Barnett Shale, the principal source of gas in the prolific Newark East Field is interpreted as being from secondary cracking of oil and bitumen (Jarvie et al., 2001).

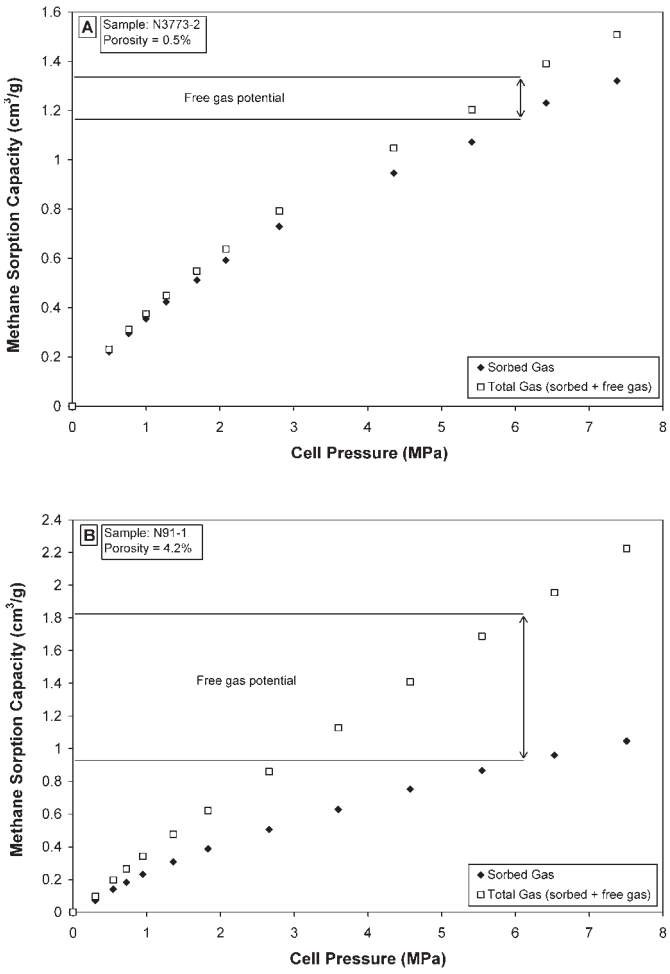

Fig. 14. Effect of porosity on potential free gas capacity. A) 0.5% porosity, free gas comprises 5% of total gas. B) 4.2% porosity increases free gas component to 70% of total gas.

Producibility

Fracturing of a gas shale reservoir (either natural or induced) is a critical factor in controlling the economic production of shale gas. Fractures in low permeability mudrocks and shales assist the flow of gas into a well and increase the volume of shale drained by a single wellbore. Due to the brittle nature of quartz (enhances fracturing), the mapping of organic-rich, siliceous-rich units has proven important for identifying gas shale 'sweet-spots' (e.g. Barnett Shale with greater than 45% quartz; Lancaster et al., 1993).

X-ray fluorescence (XRF) and x-ray diffraction (XRD) analysis of the Gordondale Member reveals that TOC contents are highest in silica-rich intervals. Unit C, composed of up to 70% quartz and 21% TOC (Ross and Bustin, 2006), has the highest potential of the Gordondale Member. High silica correlates with high Young's Modulus and low Poisson's ratio and hence mechanical properties most amenable to fracturing and the existence of natural fractures (e.g. Nygård et al., 2006). The

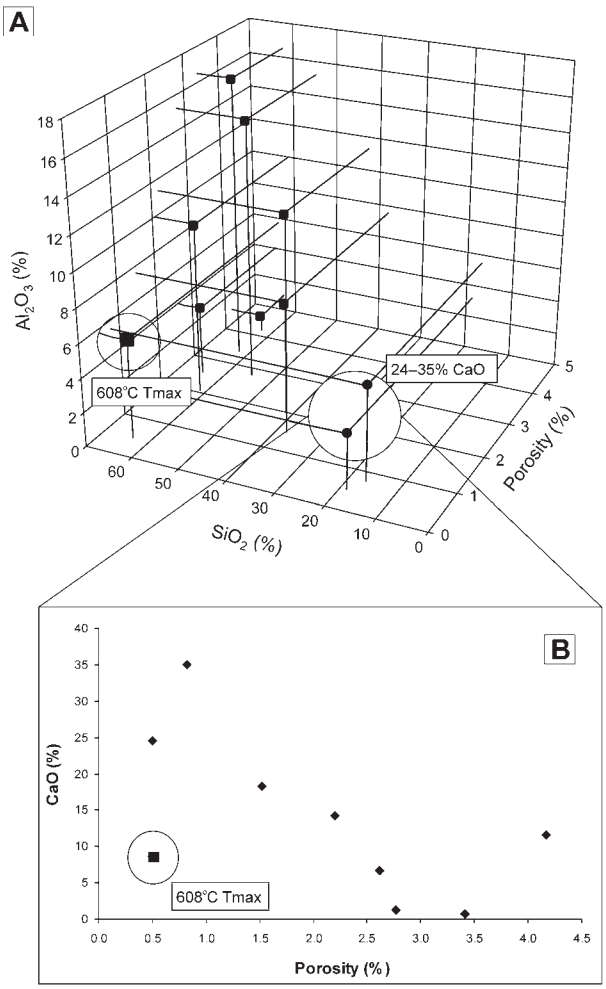

Fig. 15. Influence of the inorganic fraction on total mudrock porosity. A) Gordondale samples with more Al_2O_3 (clay minerals) have higher total porosity. The relationship between clays and porosity is affected by carbonate content (see B) and maturity [high Si, high maturity (608ºC Tmax) sample highlighted] — see text for further discussion. B) Moderate inverse relationship between carbonate (acting as cement?) and porosity.

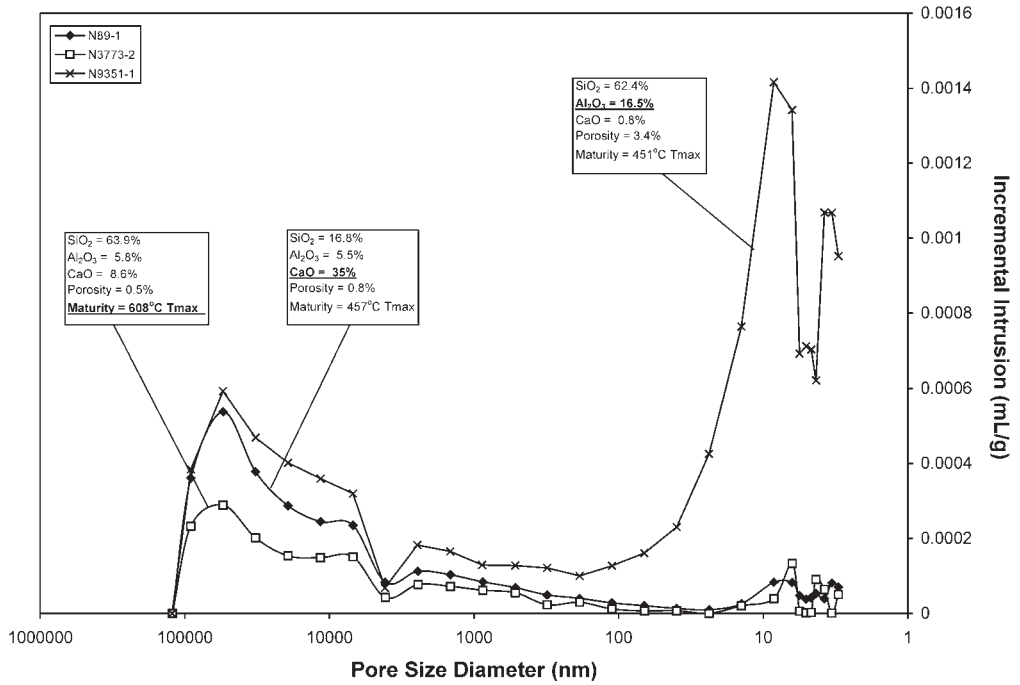

Fig. 16. Mercury pore-size distributions of Gordondale samples with various inorganic compositions. Tight mudrocks (high carbonate or thermally-mature Si-rich samples) do not show meso-micro pore-sizes due to the inability of mercury to penetrate those pores, as highlighted by low levels of Hg incremental intrusion on the Y-axis.

low amount of carbonate and expandable clay minerals such as smectite in unit C also suggests that induced fracturing may be more effective in the central sections of the Gordondale Member, coinciding with higher TOC contents and increased levels of gas sorption.

Gas production from shale reservoirs is generally considered to be hampered by the presence of multi-phase fluids (e.g. Montgomery et al., 2005). Overmature regions of the Gordondale such as in the southwest of the study area thus present better exploration opportunities due to the very low preservation potential of oil.

Gordondale Lateral Extent, Thickness and Depth

The Gordondale Member extends over an area of about 90,000 km^2 in NE BC and adjacent parts of Alberta (30,000 km^2 in NE BC). The lower (unit B) and middle Gordondale Member units (unit C) have maximum thicknesses between 11 and 13 m and are thickest along a NW–SE striking depocentre (Fig. 20). Upper Gordondale Member (unit D) is typically between 5 and 6 m thick but can reach 10 m thickness in the east-southeast of the study area. The total Gordondale Member has a thickness between 22 and 25 m, being thickest along the NW–SE region and markedly thins to the northeast due to sub-Cretaceous erosion. Some areas of the Gordondale show closed-isopach contours which may have been caused by compaction of underlying sediments, creating subsidence over the ancient axis of the Peace River Arch (Poulton et al., 1990).

A regional structure map of the Gordondale Member shows a predominant dip to the southwest (Fig. 21) — a result of thrust loading from the Laramide Orogeny (Cant, 1988) and reservoir depths range between –300 m sub-sea to below –2200 m sub-sea (over 3000 m total vertical depth; TVD) in the southwest (NTS 93-P).

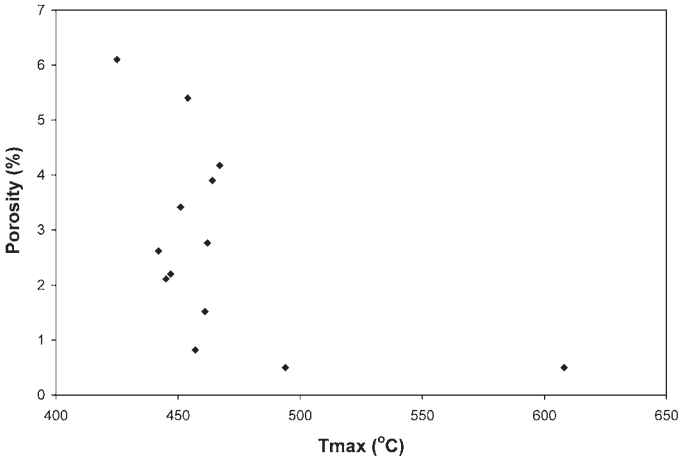

Fig. 17. Porosity vs. Tmax (used as a proxy for paleo-depth). Most samples are below 470ºC Tmax and have a wide-range of porosities which is a reflection of the different mudrock composition.

Total Gas-In-Place (GIP) Across Study Area

Total organic carbon data (Ross, 2004) has been combined with adsorption capacities (in the range of 0.1–2 cm^3/g) derived from various samples to produce a gas capacity map

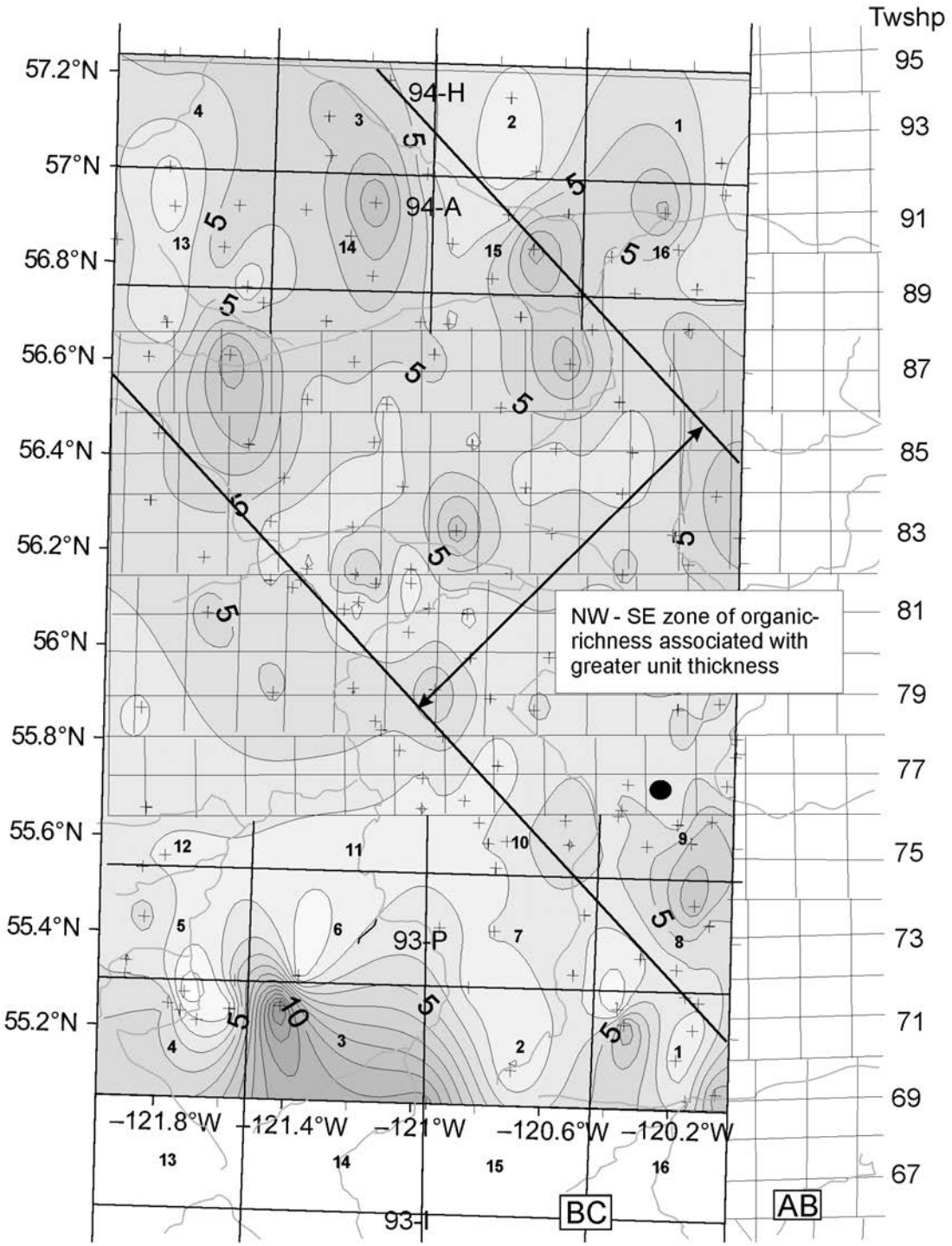

Fig. 18. Total organic carbon map of the Gordondale Member (expressed as weight percent — adapted from Ross, 2004). Enrichments of organic matter are located in two regions: 1) along the northwest/southeast elongate depocentre (from 93-P-08 to 94-H-04); and 2) in the south/southwest (93-P-03).

(combining sorbed gas capacities with free gas contents) for units B, C and D of the Gordondale Member. Reservoir pressures have been assumed to be hydrostatic for the purpose of reservoir evaluation and free gas contents calculated using an average 3% porosity and water saturation = 0%.

Unit B has potential total gas content between 1.7–13.5 Bcf/section. Larger gas capacities are associated with high TOC enrichments and greater thickness (central and south parts of study area; Fig. 22). Unit C has a high gas capacity due to elevated TOC levels and thickness yielding gas contents that

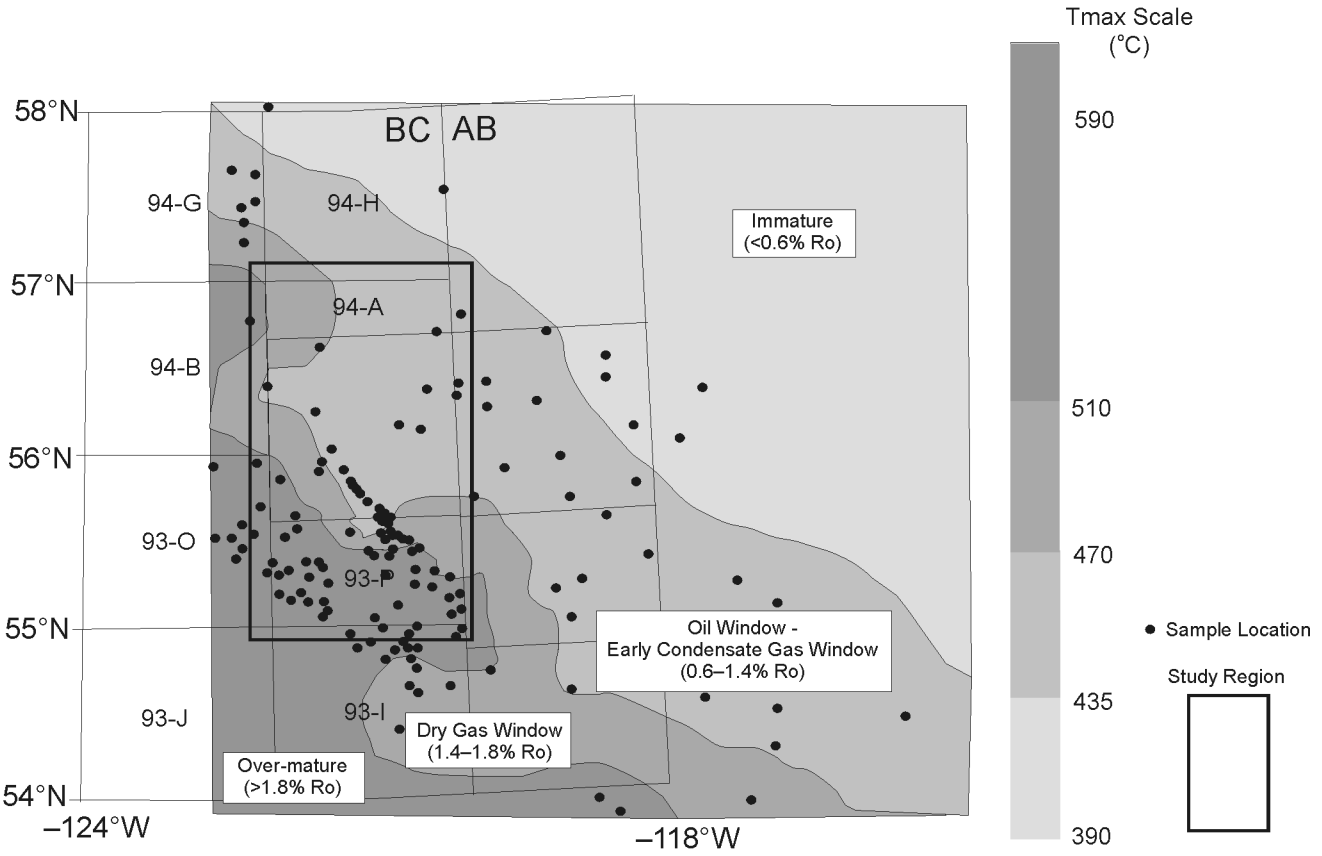

Fig. 19. Map outlining thermal maturation variability of the Gordondale Member in NE BC (adapted from Bustin, 1990). Tmax increases to the southwest, associated with greater depth of burial.

range between 1.4–21.6 Bcf/section. Unit D has the lowest gas-in-place calculated primarily due to its thinness (<7 m), ranging between 1.6–11.5 Bcf/section.

For the entire Gordondale Member, total gas capacities in the NE part of the study area range between 0.2–6.4 Bcf/section and the sorbed gas component accounts for up to 70% of the total gas content in this region (Fig. 23). Gas capacities improve to the south, associated with higher TOC contents and greater unit thickness. In particular, the south/southeast region has greater shale gas potential due to greater thermal maturation and reservoir pressures which potentially reach up to 28 MPa and as such, a larger proportion of the capacity is free gas (non-sorbed gas). The free gas component potentially comprises a significant proportion of the total gas capacity, especially at greater reservoir depths due to higher temperatures (see Yee et al., 1993). With increasing temperature, gases can overcome the weak, physical adsorption energy on surfaces and methane will fill open pores rather than being sorbed (Yee et al., 1993). Free gas can constitute up to two thirds of the total gas capacity in the south/southeast region (potentially 8.6 Bcf/sec sorbed gas and 23 Bcf/sec free gas) and during initial production stages, the gas recovered will be free gas. For comparative purposes, canister desorption data from the Barnett Shale indicates between 40 to 80% of the total gas capacity is free gas (Montgomery et al., 2005; Bustin, 2006), proving that consideration of the sorbed phase only is inaccurate for shale gas capacity.

Conclusions

I: Controls on gas capacities

1) Poor-moderate positive correlation between TOC and adsorption indicates gas adsorption capacities are influenced by TOC content, with methane adsorbing onto the organic fraction.

2) The relationship between TOC and gas sorption is complicated by the presence of moisture. Sorbed gas capacities are lower for moisture-equilibrated samples compared to the same sample in the dry-state, emphasising the ability of water to occupy potential sorption sites. Methane capacities of dry samples are of limited practical use as they do not represent in-situ reservoir conditions.

3) Sorbed gas capacities are dependent on the level of thermal maturation. With comparable organic and moisture contents, mudrock samples can have significantly larger sorbed gas capacities with greater thermal maturity.

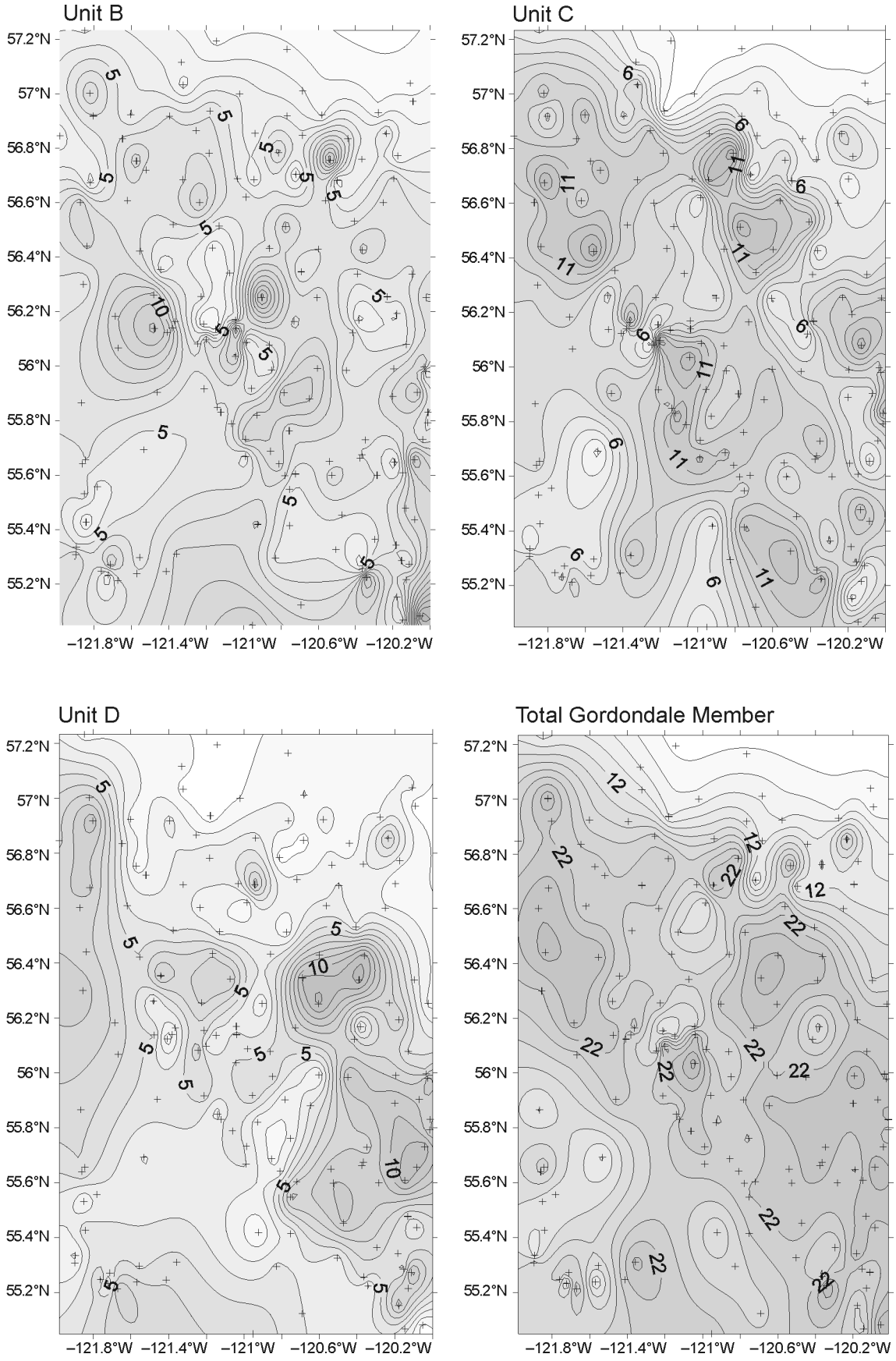
Unit B
Unit C
Unit D
Total Gordondale Member
57.2°N
57°N
56.8°N
56.6°N
56.4°N
56.2°N
56°N
55.8°N
55.6°N
55.4°N
55.2°N
−121.8°W
−121.4°W
−121°W
−120.6°W
−120.2°W

4) The inorganic fraction (primarily quartz, calcite and clays) play an important role on gas capacities in Gordondale Member and Poker Chip Shale samples. Mudrock and shale samples with greater aluminosilicate fraction (clays) have higher equilibrium moisture contents, subsequently reducing sorbed gas capacities. However clays and detrital quartz also provide a large proportion of the total open porosity, in which free gas can reside, increasing total gas capacities. An 'ideal' amount of clays in a shale gas reservoir needs to be sought for a balance between moisture contents (detrimental to gas capacities and production) and total porosity (beneficial for total gas capacities).

5) Free gas capacities can potentially be reduced through porosity reduction due to calcite cementation and burial. Therefore mudrock/shale diagenesis, as well as original bulk composition, must be taken into consideration for gas shale reservoir evaluation. Further research on a wider range of shale/mudrock samples is required to better understand the effect of diagenesis and inorganic composition on total open porosity.

II: Gordondale Gas Shale Reservoir Potential

1) The Gordondale Member has shale gas potential in NE BC due to its organic content (TOC contents between 0.8–22 weight percent), inorganic composition and thermal maturity. Of the three major units, unit C has the greatest reservoir potential due to organic-enrichment and quartz content. The positive relationship between TOC and quartz content suggests a biogenic source of the silica (unit C).

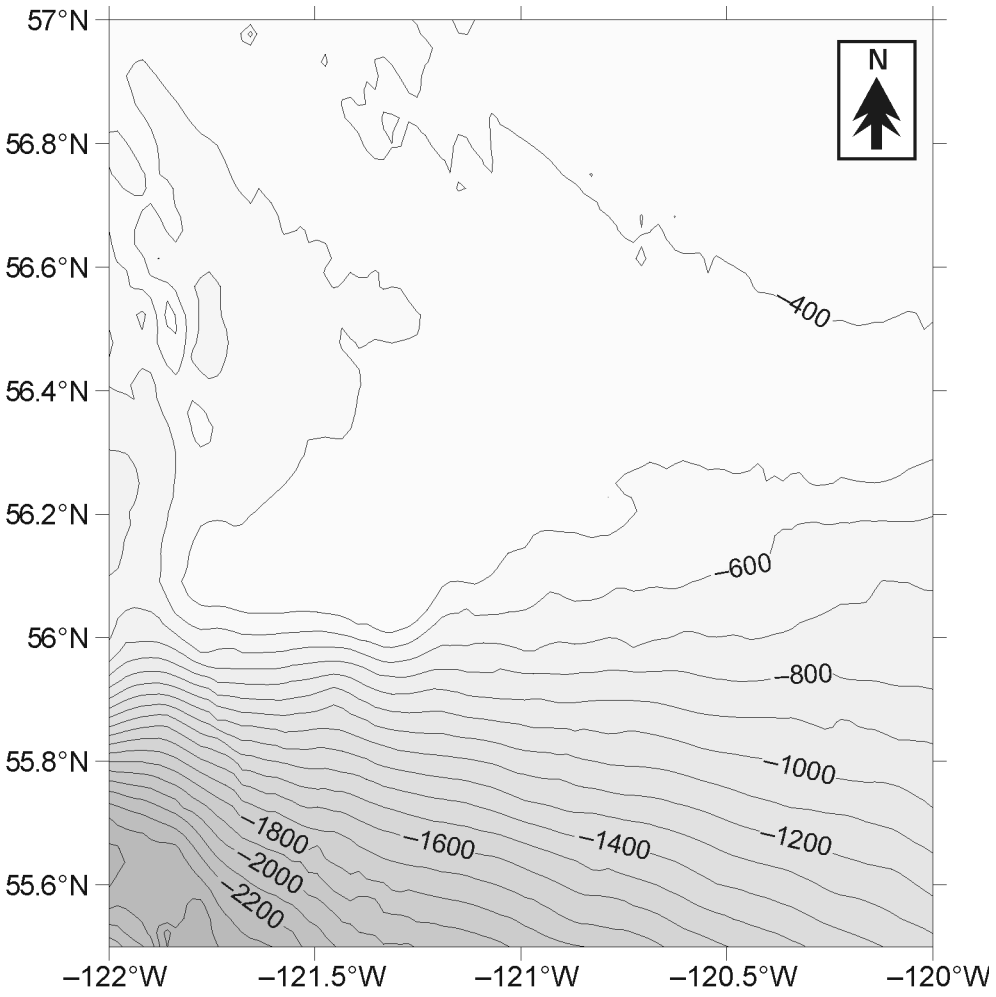

Fig. 21. Structure map to the top surface of the Gordondale Member showing increased burial depth towards the southwest of the study area (unit = metres). Depths range from –400 m sub sea-level to below –2200 m sub sea-level.

Fig. 20. Isopach maps of the shale gas units and total Gordondale Member (units are metres and control points shown as crosses). Note rapid thinning in the northeast of the study area (<6 m in 94-H-01 and 94-H-02) towards the sub-Cretaceous erosional front.

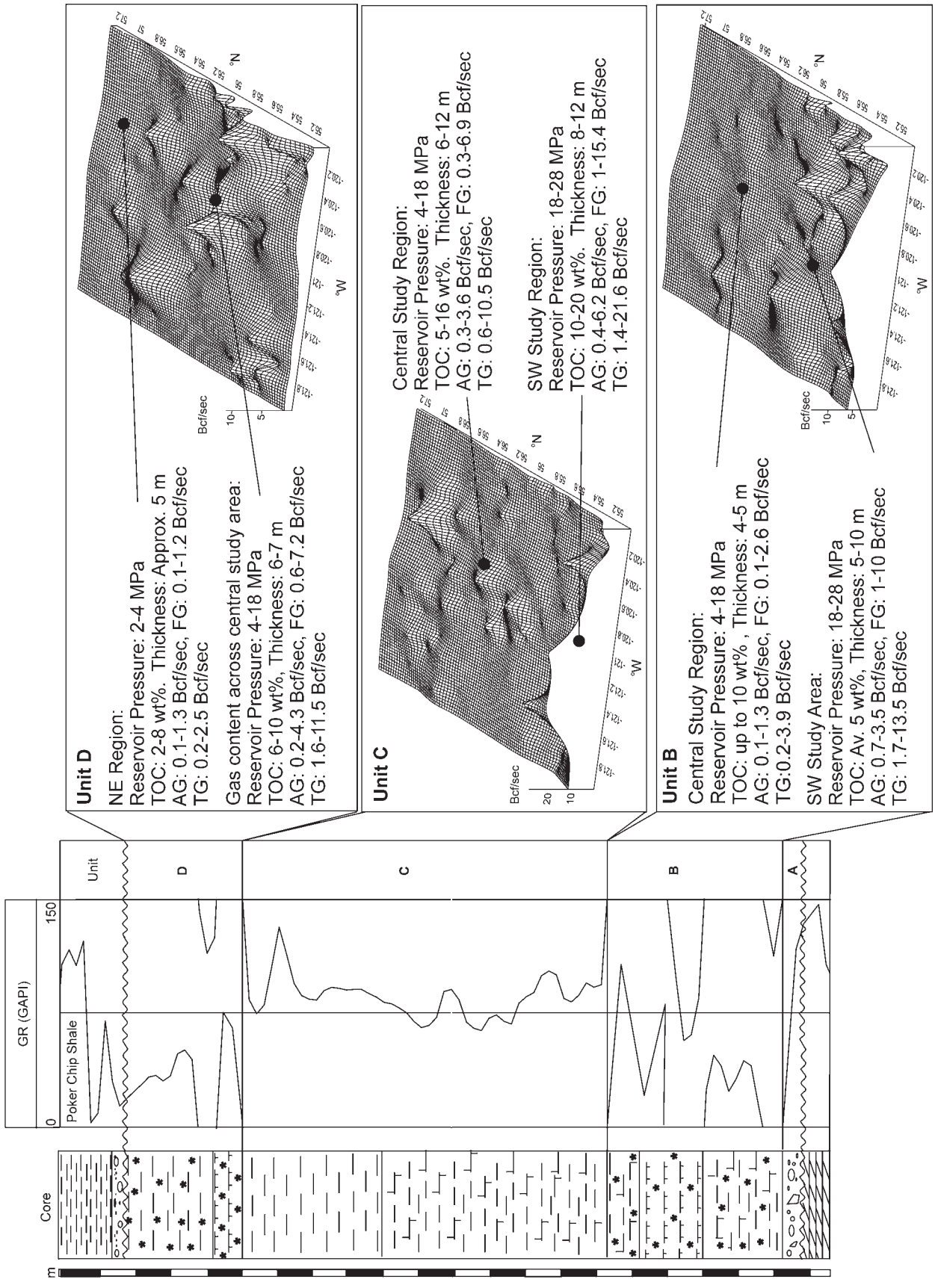

Fig. 22. Bcf per section maps for units B, C and D across study area, Core scale in metres, GR=Gamma-ray measured in API. AG=adsorbed gas; FG=free gas; TG=total gas; TG=AG+FG. Free gas calculated using 3% average porosity.

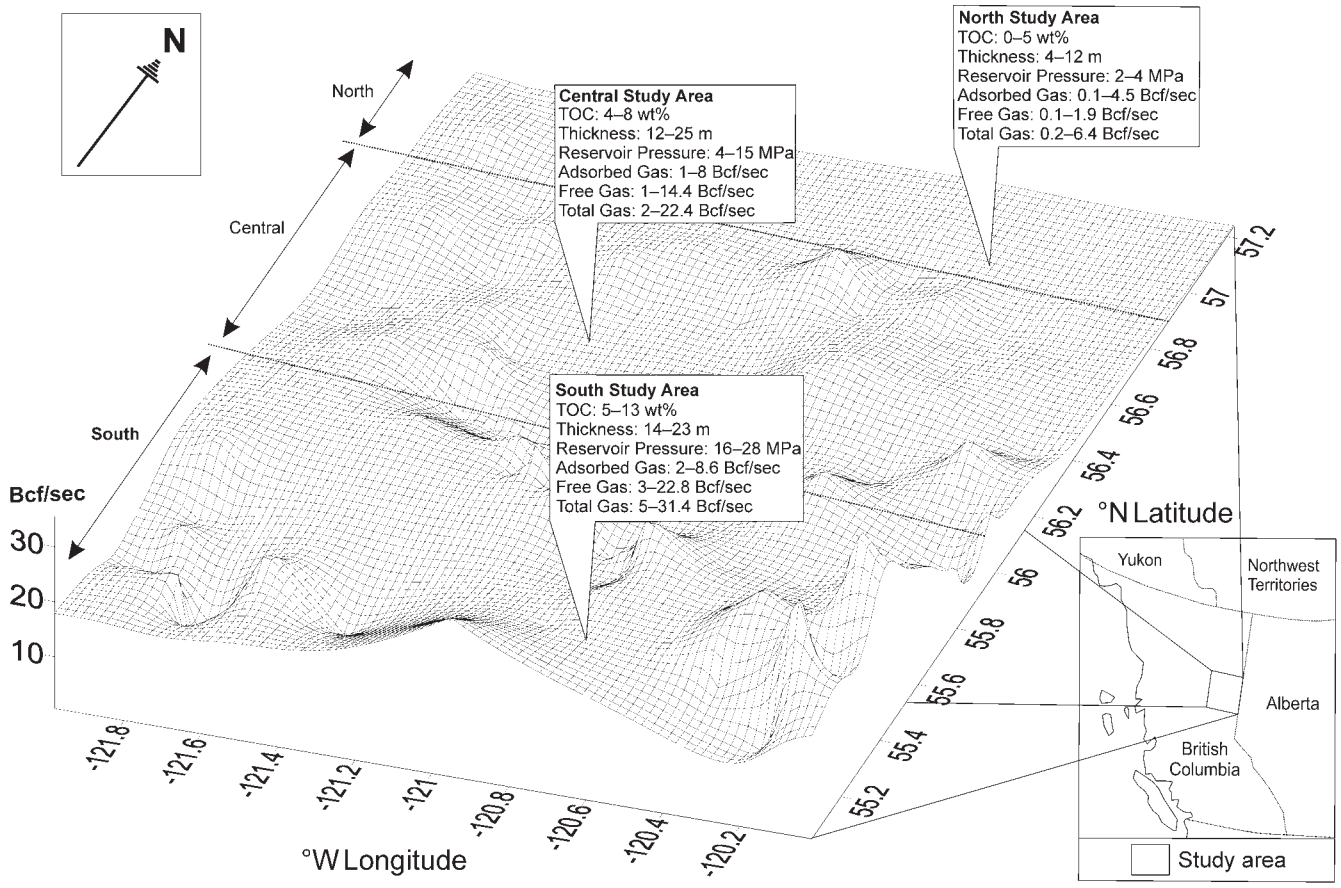

Fig. 23. Bcf per section map for total Gordondale Member in NE BC.

2) Greatest reservoir thickness is located in an elongate northwest/southeast depocentre, reaching a maximum thickness of 25 m. Total organic carbon concentrations and thermal maturation improve to the south (dry gas window – overmature in NTS 93-P), increasing the potential gas shale reservoir capacity in this region. In the southeast region of the study area, the siliceous unit C is thickest, enhancing fracturing potential of large gas capacity zones in this area.

3) Higher maturity levels to the south are also associated with greater burial depths. Therefore consideration has to be given to increased drilling costs and higher reservoir temperatures in these regions.

Acknowledgments

The authors would like to gratefully acknowledge the financial assistance of the NSERC research grant (Bustin) and CBM Solutions. Drs. Keith Dewing, Lavern Stasiuk and Glen Stockmal are thanked for their reviews and comments of the manuscript. Drs. Cynthia Riediger and Basim Faraj are thanked for reviewing an earlier version of the manuscript.

References

ASTM. 2004. Test for Equilibrium Moisture of Coal at 96 to 97% Relative Humidity and 30ºC, D1412-04, 5 p.

Aplin, A.C., Yang, Y. and Hansen, S. 1995. Assessment of β, the compression coefficient of mudstones and its relationship with detailed lithology. Marine and Petroleum Geology, v. 12, p. 955–963.

Asgar-Deen, M., Hall, R., Craig, J. and Riediger, C.L. 2003. New biostratigraphic data from the Lower Jurassic Fernie Formation in the subsurface of west-central Alberta and their stratigraphic implications. Canadian Journal of Earth Sciences, v. 40, p. 45–63.

_____, Riediger, C. and Hall, R. 2004. The Gordondale Member: designation of a new member in the Fernie Formation to replace the informal "Nordegg Member" nomenclature of the subsurface of west-central Alberta. Bulletin of Canadian Petroleum Geology, v. 52, p. 201–214.

Brunauer, S., Deming, L.S., Deming, W.S. and Teller, E. 1940. On a theory of van der Waals adsorption of gases. The Journal of the American Chemical Society, v. 62, p. 1723–1732.

Bustin, R.M. 1990. Organic Maturity in the Peace River Arch Area in the Western Canadian Sedimentary Basin. 7th Annual Meeting of The Society of Organic Petrology, Calgary, Alberta, 37 p.

_____ 2005. Gas shale tapped for big play. American Association of Petroleum Geologists, Explorer, February 2005, available online at http://www.aapg.org/explorer/divisions/2005/02emd.cfm.

_____ 2006. Rethinking Methodologies of Characterizing Gas In Place in Gas Shales. AAPG Annual Meeting, Houston, Texas. Programs and Abstracts CD, #06088.

Byørlykke, K. 1999. Principal aspects of compaction and fluid flow in mudstones. In: Muds and Mudstones: Physical and Fluid Flow Properties. A.C. Aplin, A.J. Fleet and J.H.S. Macquaker (eds.). Geological Society, London, Special Publications, p. 73–78.

Cant, D.J. 1988. Regional structure and development of the Peace River Arch, Alberta: a Paleozoic failed-rift system? Bulletin of Canadian Petroleum Geology, v. 36, p. 284–295.

Chalmers, G.R.L. and Bustin, R.M. 2007. On the effects of petrographic composition on coalbed methane sorption. International Journal of Coal Geology, v. 69, p. 288–304.

Chiou, C.T. and Rutherford, D.W. 1997. Effects of exchanged cation and layer charge on the sorption of water and EGME vapors on montmorillonite clay. Clay and Clay Minerals, v. 45, p. 8–22.

Cluff, R.M. and Dickerson, D.R. 1982. Natural Gas Potential of the New Albany Shale Group (Devonian-Mississippian) in Southeastern Illinois. SPE/DOE Symposium on Unconventional Gas Recovery, Pittsburgh, PA, Paper SPE/DOE 8924, p. 21–28, May 18–21.

Dorsch, J. and Katsube, T.J. 1999. Porosity characteristics of Cambrian mudrocks (Oak Ridge, East Tennessee, USA) and their implications for contaminant transport. In: Muds and Mudstones: Physical and Fluid Flow Properties. A.C. Aplin, A.J. Fleet and J.H.S. Macquaker (eds.). Geological Society, London, Special Publications, p. 157–173.

Espitalié, J., Laporte, J.L., Madec, M., Marquis, F., Leplat, P., Paulet, J. and Boutefeu, A. 1977. Methode rapide de caracterisation des roches meres de leur potentiel petrolier et de leur degre d'evolution: Revue de l'Institute Francais du Petrole, v. 32, p. 23–42.

Ettinger, I.L., Lidin, G.D., Dmitriev, A.M. and Zhupakhina, E.S. 1958. Systematic handbook for the determination of the methane content of coal seams from the seam pressure of the gas and the methane capacity of the coal. Institute of Mining Academy, Moscow. NCB Trans. A1606/S.E.H.

Frebold, H. 1957. The Jurassic Fernie Group in the Canadian Rocky Mountains and Foothills. Geological Survey of Canada, Memoir 287, 197 p.

Gregg, S.J. and Sing, K.S.W. 1982. Adsorption, Surface Area and Porosity. Second Edition, Academic Press, New York, p. 303.

Harris, L.D., DeWitt, W. and Colton, G.W. 1978. What are possible stratigraphic controls for gas fields in Eastern Black Shale? Oil and Gas Journal, Spring 1978, p. 162–165.

Hunt, J.M. 1996. Petroleum Geochemistry and Geology. W.H. Freeman and Company, New York, 2nd ed., 186 p.

Issler, D.R. 1992. A new approach to shale compaction and stratigraphic restoration, Beaufort-Mackenzie Basin and Mackenzie Corridor, Northern Canada. American Association of Petroleum Geologists, v. 76, p. 1170–1189.

Jarvie, D.M., Claxton, B.L., Henk, F. and Breyer, J.T. 2001. Oil and shale gas from the Barnett Shale, Fort Worth Basin, Texas [abs.]. AAPG Annual Meeting, Program and Abstracts, p. A100.

Katsube, T.J. and Williamson, M.A. 1994. Effect of shale diagenesis on shale nanopore structure and implication for sealing capacity. Clay Minerals, v. 29, p. 451–461.

Laird, D.A. 1999. Layer charge influences on the hydration of expandable 2:1 phyllosilicates. Clays and Clay Minerals, v. 47, p. 630–636.

Lamberson, M.N. and Bustin, R.M. 1993. Coalbed Methane Characteristics of Gates Formation Coals, Northeastern British Columbia: Effect of Maceral Composition. The American Association of Petroleum Geologists, v. 77, p. 2062–2076.

Lancaster, D.E., McKetta, S. and Lowry, P.H. 1993. Research findings help characterize Fort Worth Basin's Barnett Shale. Oil and Gas Journal, v. 91, p. 59–64.

Langmuir, I. 1918. The adsorption of gases on plane surfaces of glass, mica and platinum. The Journal of American Chemical Society, v. 40, p. 1403–1461.

Laxminarayana, C. and Crosdale, P.J. 1999. Role of coal type and rank on methane sorption characteristics of Bowen Basin, Australia coals. International Journal of Coal Geology, v. 40, p. 309–325.

Levy, J.H., Day, S.J. and Killingley, J.S. 1997. Methane capacities of Bowen Basin coals related to coal properties. Fuel, v. 74, p. 1–7.

Lowell, S. and Shields, J.E. 1984. Powder Surface Area and Porosity. Chapman and Hall, London, 2nd ed., 234 p.

Lu, X-C., Li. F.C. and Watson, A.T. 1995. Adsorption measurements in Devonian Shales. Fuel, v. 74, p. 599–603.

Manger, K.C., Oliver, S.J.P., Curtis, J.B. and Scheper, R.J. 1991. Geologic Influences on the Location and Production of Antrim Shale Gas, Michigan Basin. SPE 21854, p. 511–519.

McCutcheon, A.L. and Barton, W.A. 1999. Contribution of mineral matter to water associated with bituminous coals. Energy & Fuels, v. 13, p. 160–165.

Montgomery, S.L., Jarvie, D.M., Bowker, K.A. and Pallastro, R.M. 2005. Mississippian Barnett Shale, Fort Worth basin, north-central Texas: gas-shale play with multi-trillion cubic foot potential. The American Association of Petroleum Geologists Bulletin, v. 89, p. 155–175.

Nygård, R., Gutierrez, M., Bratli, R.K. and Høeg, K. 2006. Brittle-ductile transition, shear failure and leakage in shales and mudrocks. Marine and Petroleum Geology, v. 23, p. 201–212.

Pecharsky, V. K. and Zavalij, P.Y. 2003. Fundamentals of Powder Diffraction and Structural Characterization of Minerals. Kluwer Academic Publishers, New York, 713 p.

Peters, K.E. 1986. Guidelines for evaluating petroleum source-rock using programmed pyrolysis. American Association of Petroleum Geologists, v. 70, p. 318–329.

Pollastro, R.M., Hill, R.J., Jarvie, D.M. and Henry, M.E. 2003. Assessing undiscovered resources of the Barnett-Paleozoic total petroleum system, Bend Arch-Fort Worth Basin Province, Texas. Search and Discovery Article #10034, p. 1–17.

Poulton, T.P., Tittemore, J. and Dolby, G. 1990. Jurassic strata of northwestern (and west-central) Alberta and northeastern British Columbia, Bulletin of Canadian Petroleum Geology, v. 38A, p. 159–175.

Ramos, S. 2004. The effect of shale composition on the gas sorption potential of organic-rich mudrocks in the Western Canadian Sedimentary Basin. Unpublished MSc Thesis, University of British Columbia, Vancouver, British Columbia, 63 p.

Riediger, C.L. 1991. Lower Mesozoic hydrocarbon source rocks, Western Canadian Sedimentary Basin. Unpublished Ph.D. Thesis, University of Waterloo, Waterloo, Ontario, 602 p.

_____ 2002. Hydrocarbon source rock potential and comments on correlation of the Lower Jurassic Poker Chip Shale, west-central Alberta. Bulletin of Canadian Petroleum Geology, v. 50, p. 263–276.

_____ and Coniglio, M. 1992. Early diagenetic calcites and associated bitumens in the "Nordegg Member": implications for Jurassic paleogeography of the Western Canada Sedimentary Basin. Bulletin of Canadian Petroleum Geology, v. 40, p. 381–394.

_____ and Bloch, J.D. 1995. Depositional and diagenetic controls on source-rock characteristics of the Lower Jurassic "Nordegg Member". Western Canada, Journal of Sedimentary Research, v. 65A, p. 112–126.

_____, Fowler, M.G., Snowdon, L.R., Goodarzi, F. and Brooks, P.W. 1990. Source rock analysis of the Lower Jurassic "Nordegg Member" and oil-source rock correlations, northwestern Alberta and northeastern British Columbia. Bulletin of Canadian Petroleum Geology, v. 38A, p. 236–249.

Rieke, H.H. and Chilingarian, G.V. 1974. Compaction of Argillaceous Sediments. Developments in Sedimentology 16. Elsevier, Amsterdam, 217 p.

Ross, D.J.K. 2004. Sedimentology, Geochemistry and Gas Shale Potential of the Early Jurassic Nordegg Member, northeastern British Columbia. Unpublished MSc Thesis, University of British Columbia, Vancouver, British Columbia, 106 p.

_____ and Bustin, R.M. 2004. Gas Shale Potential of the Jurassic "Nordegg Member", northeastern British Columbia. CSPG Annual Meeting, Calgary, Alberta, Program and Abstracts CD, #04750128.

_____ and _____ 2006. Sediment Geochemistry of the Lower Jurassic Gordondale Member, northeastern British Columbia. Bulletin of Canadian Petroleum Geology, v. 54, no. 4, p. 337–365.

Schettler, P.D. and Parmoly, C.R. 1990. The Measurement of Gas Desorption Isotherms for Devonian Shale. GRI Devonian Gas Shale Technology Review, v. 7, p. 4–9.

Scromeda, N. and Katsube, T.J. 1993. Effect of vacuum-drying and temperature on effective porosity determination for tight rocks. Current Research, Part E. Geological Survey of Canada, Paper 93-1E, p. 313–319.

Stott, D.F. 1967. Fernie and Minnes Strata north of Peace River, Foothills of northeastern British Columbia. Geological Survey of Canada, Paper 67-19 (Part A).

Teichmüller, R. and Durand, B. 1983. Fluorescence microscopic rank studies on liptinites and vitrinites in peat and coal, and comparison with results of the Rock Eval pyrolysis. International Journal of Coal Geology, v. 2, p. 197–230.

U.S. Geological Survey. 1995. 1995 National Assessment of United States Oil and Gas Resources. Geological Survey Circular 1118. United States Government Printing Office, Washington D.C., 20 p.

Valzone, C., Rinaldi, J.O. and Ortiga, J. 2002. N_2 and CO_2 adsorption by TMA- and HDP Monrmorillonites. Material Research, v. 4, p. 475–479.

Venaruzzo, J.L., Volzone, C., Rueda, M.L. and Ortiga, J. 2002. Modified bentontic clay minerals as adsorbents of CO, CO_2 and SO_2 gases. Microporous and Mesoporous Materials, v. 56, p. 73–80.

Washburn, E.W. 1921. Note on the method of determining the distribution of pore sizes in a porous material. Proceedings of the National Academy of Science, v. 7, p. 115–116.

Webb, P.A. and Orr, C. 1997. Analytical Methods in Fine Particle Technology. Micromeritics Instrument Corporation Publishers, Norcross, p. 161–162.

Yee, D., Seidle, J.P. and Hanson, W.B. 1993. Chapter 9, Gas sorption on Coal Measurements and Gas Content. In: Hydrocarbons from Coal. B.E. Law and D.D. Rice (eds.). American Association of Petroleum Geologists, AAPG Studies in Geology, p. 203–218.

Manuscript received: September 27, 2006

Date accepted: December 15, 2006

Associate Editor: Vern Stasiuk